JVI Accepted Manuscript Posted Online 19 February 2020
J. Virol. doi:10.1128/JVI.01597-19

Identification of host trafficking genes required for HIV-1 virological synapse formation in dendritic cells

Rebecca Bayliss[1], James Wheeldon[1,] Stephan M Caucheteux[2], Carien M Niessen[3], Vincent Piguet [1, 4, 5*]

[1] Division of Infection and Immunity, School of Medicine, Cardiff University, Cardiff, CF14 4XN, UK.

[2]Department of Medicine, University of Toronto, Toronto; M5S 1A8, Canada

[3]Department of Dermatology, Cologne Excellence Cluster on Cellular Stress Responses in Aging Associated Diseases (CECAD), and Center for Molecular Medicine, University of Cologne, 50931 Cologne, Germany.

[4] Division of Dermatology, Women's College Hospital, Toronto; M5S 1B2, Canada

[5] Division of Dermatology, Department of Medicine; University of Toronto, Toronto; M5S 1B2, Canada

*Correspondence/Lead: vincent.piguet@utoronto.ca

ABSTRACT

Dendritic cells (DC) are one of the earliest targets of HIV-1 infection acting as a 'Trojan Horse', concealing the virus from the innate immune system and delivering it to T-cells via virological synapses (VS). To explicate how the virus is trafficked through the cell to the VS and evades degradation, a high-throughput siRNA screen targeting membrane trafficking proteins was performed in monocyte-derived dendritic cells (MDDC). We identified several proteins including BIN-1 and RAB7L1 that share common roles in transport from endosomal compartments. Depletion of target proteins resulted in an accumulation of virus in intracellular compartments and significantly reduced viral *trans*-infection via the VS. By targeting endocytic trafficking and retromer recycling to the plasma membrane, we were able to reduce the virus's ability to accumulate at budding microdomains and the VS. Thus, we identify key genes involved in a pathway within DC that is exploited by HIV-1 to traffic to the VS.

IMPORTANCE

The lentivirus Human Immunodeficiency Virus (HIV) targets and destroys CD4+ T-cells, leaving the host vulnerable to life-threatening opportunistic infections associated with Acquired Immunodeficiency Syndrome (AIDS). Dendritic cells form a Virological synapse (VS) with CD4+ T-cells, enabling the efficient transfer of virus between the two cells. We have identified cellular factors that are critical in the induction of the VS. We show that ARF1, BIN1, RAB7L1 and RAB8A are important regulators of HIV-1 trafficking to the VS and therefore infection of CD4+ T-cells. We

found these cellular factors to be essential for endosomal protein trafficking and formation of the VS, depletion of target proteins prevented virus trafficking to the plasma membrane by retaining virus in intracellular vesicles. Identification of key regulators in HIV-1 trans-infection between DC and CD4+ T-cells has the potential for development of targeted therapy to reduce trans-infection of HIV-1 in *vivo*.

INTRODUCTION

Dendritic cells (DC) are key antigen-presenting cells that provide an important link between innate and adaptive immune systems, activating T-cells (reviewed in (1, 2)). Although HIV-1 is able to replicate in DC, the process is inefficient and produces low levels of infectious virus (3-8). However, DCs are able to transfer intact viral particles to target T-cells via a virological synapse (VS) by a process termed *trans*-infection (9), contributing to the spread of infection *in vivo* (10, 11).

HIV-1 *trans*-infection has been shown to depend on the ability of the virus to 'surf' along the surface of the DC via actin rich dendrites, to promote *trans*-infection (12-14). Several studies conducted in macrophages and DC located virus sequestered into plasma membrane invaginated compartments from which viral particles are released at the VS (15-18). These compartments are thought to be surface accessible (15), however there is evidence of a population becoming isolated from the cell surface (16). It is established in macrophages and DC that these surface accessible compartments may have complex morphologies that require membrane

trafficking regulation, such as the virus containing compartments found in macrophages (17).

In contrast, c*is*-infection of DC is limited by the host restriction factor SAMHD1, a dinucleotide triphosphate (dNTP) hydrolase that blocks reverse transcription of viral DNA (19-24). In addition, viral cytosolic DNA is sensed by cGAS, a GMP-AMP synthase that induces an interferon type I response in DC (25-27) restricting productive viral replication.

It has been previously reported that HIV-1 virus enters the cell through the endolysosomal pathway with evidence supporting roles for clathrin-mediated endocytosis (4, 28, 29), receptor-mediated endocytosis (30, 31) and macropinocytosis (32). However, at later time points virus accumulates in virus containing compartments, rich in tetraspanins such as CD81 that are continuous with the plasma membrane (4, 15, 17). More recent studies identified the importance of tetraspanin 7 (TSPAN7) and dynamin 2 (DNM2) in maintaining viral particles on dendrites and promoting efficient viral transfer. Disruption of these targets led to sequestration of virus in intracellular vesicles and a reduction in viral transfer (13).

To elucidate the role of membrane trafficking in the capture and trafficking of the virus through DC to the VS, we performed a high-throughput siRNA screen targeting membrane trafficking proteins. Our results identified proteins involved in vesicle trafficking between early endosomes, the trans-Golgi network (TGN) and the plasma membrane that reduce transfer of HIV-1 from DC to T-cells. We show that HIV-1 is dependent on a functioning endocytic pathway, disruption of which results in an accumulation of virus in intracellular vesicles, blocking trafficking of the virus to the virological synapse.

RESULTS

siRNA membrane trafficking library identified genes involved in HIV-1 *trans*-infection between DC and T-cells.

To identify the cellular trafficking pathways involved in the transfer of HIV-1 in *trans*-infection from DC to CD4+ T-cells, a siRNA library targeting 140 membrane trafficking genes was utilised. SMARTpool siRNA were transfected into MDDC 48 hours before infection with full-length CXCR4-tropic HIV-1 (R9) and co-cultured with SUPT1 cells at 1:1 ratio. HIV-1 infected SUP-T1 cells were analysed by flow cytometry 48 hours later. No infection was detected in SUP-T1 cells inoculated with a HIV-1 fusion-mutant control (Figure 1a). Non-target siRNA were used to compare infection levels and showed < 20% variation between replicates (Z score = 1.5 s.d.), therefore the lower assay cut-off point was set at 20%.

In the primary screen, the knockdown of 16 genes induced a reduction in HIV-1 *trans*-infection greater than or equal to 20%, whereas 25 genes showed an increase in viral *trans*-infection by over 50% (Figure 1b). The primary Hits were reproduced in two donors using autologous CD4+ T-cells activated with IL-2 and PHA. Nine Hits showed a reproducible reduction in HIV-1 transfer: *AP1M1, AMPH1, ARF1, BIN1, EPN3, PAK1, RAB7L1, RAB8A and WASF1* (Figure 1c). Hits that resulted in an increase in HIV-1 transfer included *AP2M1, CLTB, CLTC, EPS15, GRB2, HIP1, RAB1A, RAB2, ROCK1, VAV2, EFS, MAPK8IP2, DNM3* (Figure 1d).

Efficient HIV-1 *trans*-infection requires vesicle trafficking at the plasma membrane

To understand potential relationships between the genes selected in the siRNA screen, gene-annotation enrichment analysis was used to identify common

interactions between the candidate genes that may be involved in the *trans*-infection of HIV-1 between DC and T-cells. Analysis of the siRNA candidates was carried out for cellular compartments and biological processes (Table 1). Our results show that the genes required for optimal viral transfer are primarily involved in endocytic compartment regulation, whereas genes that restrict viral transfer are largely involved in clathrin-coat mediated endocytosis and actin-dependent processes at the plasma membrane. Taken together the data suggests that preventing viral uptake via clathrin coated vesicles enhances viral transfer, which is likely due to increased retention of virus on the cell surface. This finding is in agreement with studies that show HIV-1 transmitted in *trans* between DC and T-cells from the surface of DC (12, 13). In contrast, genes required for efficient *trans*-infection are strongly associated with cytoplasmic membrane bound vesicles and vesicle-mediated transport supporting the view that HIV-1 is sequestered into intracellular virus-containing compartments (VCC) (15, 16, 33).

ARF1, BIN1, RAB7L1 and _RAB8A_ are required for HIV-1 _trans_-infection

The siRNA library used to identify target genes is comprised of a set of four separate siRNA sequences which target different regions of the same gene; these are pooled to reduce the potential off-target effects of siRNA transfection. The knockdown of the pooled siRNA typically reflects the most functional siRNA within the pool. Therefore, the four individual siRNA can be analysed for their ability to reduce viral transfer to validate whether the observed phenotype is a genuine on-target effect.

The main aim of our study was to identify cellular pathways involved in the delivery of HIV-1 to the VS to aid *trans*-infection; therefore, we focused our investigation on the genes that facilitate the transfer of HIV-1 between DC and T-cells. Each of the four siRNA were transfected individually into MDDC, infected with HIV-1 (R9) and co-cultured with autologous T-cells for 48 hours. Of the final nine candidates, three showed a reduction in transfer (≥20%) in at least two of the four individual siRNA, across four independent donors: *BIN1* (siRNA B and C), *RAB7L1* (siRNA A, C and D) and *RAB8A* (siRNA A, and B) (Figure 2a). An average reduction of 50% in transfer was evident for ARF1 siRNA A, whereas ARF1 siRNA B produced a 17-20% knockdown in viral transmission in 3 out of the 4 donors analysed. Thus, in conjunction with the targeted reduction of ARF1 at the protein level, this result indicates that ARF1 siRNA A was the most functional siRNA in the pool and it was therefore decided to pursue this candidate further.

To determine the level of protein depletion in MDDC, cell lysates transfected with 200 nM pooled siRNA (Figure 2b) targeting the entire length of the gene were analysed by western blot. Knockdown was quantified by densitometry relative to protein expression levels in non-target siRNA transfected lysates. An efficient knockdown was achieved using pooled siRNA, 35% (± 17) reduction of protein expression was observed for ARF1, 52% (± 6.6) for BIN1, 53% (± 23.4) for RAB7L1 and 54% (± 8.1) for RAB8A compared to non-target siRNA (Figure 2c).

To confirm whether siRNA is capable of reducing viral *trans*-infection independent of viral strain, MDDC were transfected with the selected target siRNA and infected with either R8BAL (CCR5-tropic) and R9 (CXCR4-tropic) HIV-1. A significant reduction in viral transfer - ranging between 26-40% in R9 infected cells

and 35-45% in R8BAL infected cells - was observed for all candidates demonstrating that host factors involved in trafficking to the VS are shared for both CXCR4- and CCR5-tropic strains of HIV-1 (Figure 2d and e). All MDDC transfected with pooled siRNA remained > 80% viable compared to control cells, ensuring that the reduction in transfer is not due to cellular toxicity of the siRNA transfection (Figure 2f). Further, siRNA transfection of MDDC resulted in a marginal (< 5%) increase in DC maturation marker CD83. Viral binding of p24 Gag also saw a marginal increase compared to untreated and mock transfected cells, however HIV-1 internalisation was not affected confirming the observed reduction in *trans*-infection is not due to decreased binding or internalisation of the virus (data not shown).

Future experiments were conducted on selected candidate siRNA showing evidence of protein knockdown and a reduction in viral *trans*-infection in at least two of the four individual siRNA tested. siRNA candidate genes that failed to meet these criteria (WASF1, EPN3, PAK1, and AMPH1) showed no evidence of a reduction in viral *trans*-infection when MDDC were transfected with individual siRNA nor were we able to detect a specific knockdown in protein expression, suggesting the previously observed reduction in viral trans-infection maybe due to off-target effects of those specific siRNA. Therefore, these genes were eliminated from further analysis along with AP1M1 which showed high variability in the reduction of viral transfer between donors. The final candidates included ARF1, associated with retrograde transport at the Golgi and protein transport to endosomes (34, 35), BIN-1, known to form a complex with dynamin to control vesicle transport and scission (36), RAB7L1 a GTPase required for retromer recycling between the TGN and endosomes (37) and

184 GTPase RAB8A involved in polarised vesicular trafficking to the plasma membrane
185 from TGN (38).
186
187 **Depletion of target proteins reduces virological synapse formation between MDDC**
188 **and CD4+ T-cells.**
189 The efficient *trans*-infection of HIV-1 from DC to T-cells is dependent on the
190 formation of VS, an adhesive structure that promotes viral transmission (39, 40). To
191 assess if the observed reduction in *trans*-infection was due to a reduction in VS
192 formation, siRNA transfected MDDC were infected with HIV-1 R9 or R8BAL and co-
193 cultured with autologous CD4+ T-cells. Imaging of the transfected MDDC revealed
194 that in the case of *BIN1* and *RAB7L1* siRNA transfected cells, HIV-1 R9 appeared to
195 accumulate in large cellular vesicles at the plasma membrane and did not form VS
196 with the T-cells in spite of apparent interactions between the two cell types. In
197 addition, *ARF1* and *RAB8A* depleted cells also appear to inhibit VS formation;
198 however, accumulation of virus can be seen in smaller vesicles at the cell periphery
199 (Figure 3a). Quantification of VS was similar in non-target siRNA, untreated and mock
200 transfected cells. All candidate siRNA had a 40-60% reduction in VS formation
201 between DC and T-cells when compared to non-target siRNA transfected cells (Figure
202 3b). Similar results were seen for R8BAL infected MDDC, a reduction in VS number
203 with T-cells was observed, however *BIN1* and *RAB7L1* transfected cells did not
204 accumulate virus in intracellular vesicles to the extent seen in R9 infected MDDC
205 (Figure 3c, 3d). In addition, we observed that LFA-1, a stabilising component of the
206 VS, did not become enriched at the interface between the MDDC and T-cells in the
207 absence of virus (data not shown). These data suggest that virus is targeted to

cytoplasmic vesicles after entry into MDDC, however onward trafficking of virus to the plasma membrane is inhibited by depletion of the target genes, preventing VS formation and reducing efficient trans-infection between the DC and CD4+ T-cells.

The integrity of virus containing vesicles are compromised in BIN1 and RAB7L1 depleted MDDC cells.

CD81, a type II transmembrane protein, is one of the main tetraspanins recruited to the host cell membrane during HIV-1 *trans*-infection and is known to co-localize with HIV-1 containing compartments in macrophages and DC (4, 18, 41). To determine if target siRNA altered endogenous CD81 localisation in MDDC, transfected cells were labelled for CD81 (Figure 4a). In control cells (non-target siRNA) CD81 is found at the cell periphery with a faint perinuclear staining. In contrast, *ARF1* siRNA saw a reduction in CD81 positive vesicles that are evident within both the cytoplasm and at the cell periphery. *BIN-1* and *RAB7L1* depletion reduced CD81 vesicle number and size, whereas no significant difference was observed in cells depleted of RAB8A (Figure 4b-c). In all three cases, an accumulation of CD81 vesicles was observed within the cytoplasm not at the cell periphery (Figure 4a).

CD81 plays an important role in regulating viral *trans*-infection at the VS and depletion of the tetraspanin can reduce viral *trans*-infection (42). In light of previous findings, we assessed CD81 localisation during HIV-1 infection. As expected, we observed p24 Gag co-localisation with CD81 at the cell periphery in CD81 tetraspanin-enriched micro domains (TEM) at 4 hours post-infection in control cells. In transfected MDDC, we observed that the number of CD81 p24 Gag TEM's are

reduced in *ARF1* depleted cells. In contrast, cells transfected with siRNA targeting *BIN1, RAB7L1* and *RAB8A* saw both virus and CD81 at the cell periphery, however the staining of the TEM was diffuse and lacked the structure of the TEM (Figure 4d-e). This was confirmed by co-localisation data indicating that CD81 association with p24 was reduced in siRNA transfected cells (Figure 4f). Taken together, these data suggest that trafficking of CD81 and p24 Gag to the cell periphery to form the TEM is compromised by knockdown of *ARF1*, *BIN-1, RAB7L1* and *RAB8A* potentially preventing the efficient *trans*-infection of virus via the VS.

Retention of virus in endocytic compartments reduces HIV-1 transfer

We hypothesised that the presence of virus and CD81 in cytoplasmic vesicles and the disrupted trafficking of CD81 and p24 Gag to the plasma membrane by target siRNA was due to retention in endocytic compartments. Therefore, we aimed to trap virus in endosomal derived vesicles to establish if this directly affects viral *trans*-infection to T-cells. MDDC were treated with endocytic inhibitors prior to infection with R9 virus and the level of *trans*-infection was measured. We utilised LY294002, a phosphatidylinositol 3-kinase (PI3K) inhibitor known to block macropinocytosis and the formation of early endosomes, and Bafilomycin A1, a vacuolar type H^+-ATPase (V-ATPase) that prevents endosomal acidification.

Inhibition with LY294002 resulted in a mild increase of HIV-1 *trans*-infection (+ 20%) when compared to DMSO treated control cells. However, a 2-fold decrease in *trans*-infection was observed in cells treated with Bafilomycin A1, indicating that efficient viral transfer requires a functioning endocytic pathway (Figure 5a). This reduction was not due to inhibitor toxicity, with MDDC remaining > 80% viable

during treatment and subsequent infection (Figure 5b). To visualise any differences between MDDC treated with LY294002 and Bafilomycin, infected MDDC were analysed by confocal microscopy. HIV-1 was concentrated at the cell surface in cells pre-treated with LY294002, which is in agreement with previous findings (13). In contrast, virus accumulates inside intracellular vesicles in cells treated with Bafilomycin A1 (Figure 5c) indicating that viral uptake into MDDC was not inhibited, and retention within endocytic vesicles reduced *trans*-infection. Controls confirmed that both horseradish peroxidase (HRP) taken into the MDDC via fluid–phase and the lysosomal marker low-density lipoprotein (LDL) were lost in cells treated with the PI3K inhibitor LY294002, as predicted. In contrast, LDL-DiI labelling was diffuse and cytoplasmic in cells treated with Bafilomycin A1, suggesting a block in LDL-DiI uptake by endosomes in the MDDC. On the contrary, HRP taken up via fluid-phase was less affected, suggesting that unlike LDL, HRP is retained in endocytic-like compartments (Figure 5d).

HIV-1 did not co-localise with organelle markers EEA1, Rab5, Rab7, Rab11, LAMP2 or CHMP2B in either siRNA transfected or Bafilomycin A1 treated MDDC in our experiments, suggesting that these HIV-1 positive compartments may be intermediate vesicles devoid of characteristic markers.

Taken together, these data indicate that HIV-1 transfer is reliant on a functioning endocytic pathway. Blocking virus in endosomal derived compartments results in the accumulation of virus in cytoplasmic vesicles, which in turn reduces viral transfer between MDDC and T-cells, as seen in siRNA transfected MDDC. In addition, Bafilomycin A1 appears to block LDL-DIL but not HRP or HIV-1 uptake into

MDDC, suggesting that HIV-1 is predominately trafficked to cellular compartments that differ from those utilised by LDL.

Downstream trafficking from early endosomes is compromised in MDDC transfected with target siRNA

Endosomal cargo has one of two fates; it is either recycled back to the cell surface (i.e. transferrin) or directed to lysosomes for degradation (i.e. LDL). To confirm that target siRNA are blocking endosomal trafficking in MDDC, cells were transfected with pooled *ARF1, BIN-1, RAB7L1* and *RAB8A* siRNA and either stained for early endosomes with early endosome antigen 1 (EEA1), incubated with Alexa Fluor labelled Transferrin, or LDL-DIL, to assess the recycling and lysosomal trafficking pathways respectively.

In non-target siRNA transfected MDDC, EEA1 is seen in numerous vesicles of various sizes throughout the cell. MDDC transfected with siRNA against *ARF1, BIN1 and RAB8A* resulted in the formation of abnormal endosomes marked by a decrease in both number and size. *RAB8A* siRNA resulted in more numerous, enlarged vesicles evident at the cell periphery (Figure 6a-c).

In all instances labelled transferrin was found localised at the cell periphery, with no discernible differences between control and siRNA transfected cells (Figure 6a, panel 2). However, a reduction in vesicle number and Alexa Fluor labelling was observed in *BIN1, RAB7L1* and *RAB8A* transfected cells (Figure 6d-e).

In non-target siRNA or mock transfected control cells, LDL-DIL predominately accumulates in lysosomes in the perinuclear region. In cells transfected with siRNA targeting *ARF1*, LDL has accumulated in various sized vesicles in the cytoplasm

(Figure 6a, panel 3). Knockdown of *BIN-1*, *RAB7L1* resulted in a reduction of LDL containing vesicles within the cells indicating that the delivery of LDL-DIL to lysosomes is significantly reduced (Figure 6a, f-g). *RAB8A*-silenced cells were also found to have a reduced number of LDL vesicles; however, a diffuse staining is evident within the cytoplasm, suggesting that LDL is taken into the cell but not trafficked within the endolysosomal pathway.

These observations suggest *ARF1* regulates endosomal morphology and vesicle formation and slows LDL trafficking to the perinuclear region but is dispensable for the recycling of transferrin to the plasma membrane. *BIN1* and *RAB7L1* also affect endosomal vesicle formation, resulting in the retention of vesicles at the cell periphery and reducing downstream trafficking from endosomes, evidenced by a reduction in both transferrin and LDL containing vesicles suggesting *BIN1* and *RAB7L1* play a role in early endosomal protein trafficking. In contrast, RAB8A depletion appears to increase early endosome size, although trafficking of both LDL and transferrin is also reduced suggesting RAB8A actions is targeted more downstream regulating protein trafficking after cargo has left the endocytic compartment. The disruption of endosomal vesicle trafficking at or after the early endosomal compartment by target siRNA creates a knock-on effect, altering endocytic trafficking to lysosomes and recycling of cargo to the plasma membrane. Taken together, the disruption of TGN-endosomal-plasma membrane trafficking suggests that HIV-1 trafficking from internalised compartments relies of endosomal sorting pathways to traffic to and accumulate at the VS and potentially within VCC at the cell surface.

HIV-1 *trans*-infection requires retromer complex recycling of cargo

Based on the findings that trafficking between key endosomal compartments is compromised in siRNA targeted cells which in turn reduces HIV-1 trafficking to the VS - we wanted to confirm whether *trans*-infection of HIV-1 was reduced when trafficking to the plasma membrane from the TGN or early endosomes is compromised. Several of our selected genes play a key role in endosomal sorting to the TGN and plasma membrane with *RAB7L1* specifically involved in retromer activity. In addition, a proportion of transferrin and its receptor are recycled in a retromer-dependant manner to the plasma membrane (43). The retromer has also been found to play a key role in HIV-1 Env trafficking and viral assembly (44). Thus, we decided to investigate the role of the retromer complex in *trans*-infection using siRNA targeting key components of the retromer complex, VPS26A and VPS35. HIV-1 *trans*-infection was significantly reduced in MDDC transfected with each of the retromer siRNA (Figure 7a-b) from 25-50%. A more marked reduction was evident in cells infected with CXCR4-tropic strain of the virus. A protein knockdown of approximately 60% was confirmed for both VPS26A and VPS35 (Figure 7c-e), and no reduction in cell viability was evident from siRNA transfection of the VPS genes. Therefore, we were able to confirm endosomal sorting between the TGN and to the plasma membrane is required for HIV-1 *trans*-infection.

DISCUSSION

DC perform an essential role in the transmission of HIV-1 to target CD4+ T-cells promoting the spread of infection. Although there have been numerous investigations into the role of DCs in *trans*-infection, the cellular trafficking pathways

exploited by HIV-1 remain unclear. The identification of host cell factors and intracellular pathways exploited by HIV-1 to aid *trans*-infection of T-cells will facilitate the development of novel therapies and may reduce initial transmission of HIV-1.

In this study we identified a number of host factors involved in *trans*-infection of HIV-1 from DC to T-cells. By conducting a siRNA screen targeting membrane trafficking proteins we identified four genes involved in efficient *trans*-infection from DC to T-cells. Although, one similar shRNA/siRNA screen has been conducted investigating the role of membrane trafficking in HIV-1 *trans*-infection, none to date has focused on the genes we identified in the current study. In a recent shRNA screen Menager and Littman (13) also identified *ARF1, ARF6* and *ARPC1B* as reducing viral transfer and *CLTC, CLTB* and *AP2M1* enhanced viral transfer, however the ability to draw direct comparisons between the two studies is complicated by the fact that Menager uses shRNA technology in a screen that targets a different gene library, several of them not included in the siRNA screen we utilised. The study then proceeds to concentrate on TSPAN7 and DNM2 and their role in *trans*-infection at the cell surface, whereas we have focused on the trafficking of internalised virus. In a study using an identical siRNA screen, Wen *et al.* identify a number of common genes such as R*AB7L1, AP1M1, BIN-1, ARPC1B, DIAPH1, ARF6, WASF1, CLTC and VAV2* required for HIV-1 and M-PMV virus release from HeLa cells *(45).* Overall, there is a high consistency of hits between previous screens conducted in DCs and our own membrane trafficking screen, verifying our findings.

Our initial siRNA screen shows that knocking down genes associated with clathrin-coated vesicle formation enhanced *trans*-infection; this suggests that restricting viral uptake into MDDC and retention of virus on the cell surface promotes HIV-1 *trans*-infection. It has been previously demonstrated that soluble CD4 protein is able to inhibit infection therefore proposing that virus particles bound to the surface of the MDDC were the main source of *trans*-infection (12). In support of this model, Menager *et al.* demonstrated that DNM2 and TSPAN7, which coordinate actin nucleation and stabilization, had roles in restricting endocytosis and maintaining virus on cellular dendrites enabling transfer (13, 46). On the other hand, there is compelling evidence for the model that HIV-1 is sequestered in plasma membrane-derived invaginated compartments induced upon HIV-1 uptake (33). From this compartment, viral particles can be released to the VS to initiate *trans*-infection (15-17). We initially identified 9 genes from the siRNA screen that reduced *trans*-infection. These genes were predominately associated with cytoplasmic, membrane-bound vesicles with direct involvement in vesicle-mediated transport and membrane organisation, thus supporting a requirement for membrane-bound vesicles in HIV-1 *trans*-infection. These results provide evidence for both viral transmission via the cell surface and trafficking via intra-cellular compartments to promote *trans*-infection in MDDC.

Although the use of primary MDDC and CD4+ T-cells is a representative model of HIV-1 *trans*-infection, employing methods such as siRNA transfection within established MDDC has its limitations. Generally, 50% transfection efficiency is achieved, which in turn does not completely block reduction of *trans*-infection within these cells. However, partial knockdown is still capable of producing a strong

phenotype and the study of these pathways in primary cells is essential to uncovering underlying mechanisms of *trans*-infection and is critical for investigating and identifying such cellular processes.

In this study, we concentrate on studying genes required for efficient viral *trans*-infection and therefore aim to investigate how internalised virus is trafficked to the VS. We demonstrate that the reduction in viral *trans*-infection observed from depletion of four genes: *ARF1*, *BIN1*, *RAB7L1* and *RAB8A* is due to the apparent retention of virus in intra-cellular vesicles and a reduction in virus accumulation at the VS between DC and T cells. MDDC are able to capture and store HIV-1 virions in invaginations at the plasma membrane (9, 15). Live-imaging shows viral puncta are trafficked into enclosed intracellular compartments (47), whether these compartments are enclosed or remain accessible to the cell surface is still at matter of debate (15, 16). The integrity and formation of intracellular compartments are believed to be regulated by membrane trafficking processes (17). Based on this data we propose that the reduction in VS formation observed in siRNA-treated MDDC disrupts the regulation and trafficking of intra-cellular compartments resulting in the retention of viral particles within intra-cellular vesicles, preventing onward trafficking to the VS and therefore inhibiting viral *trans*-infection.

VS formation and HIV-1 spread relies on the interaction of MDDC and recipient T-cells, triggering the active polarisation of organelles and cell surface proteins. One such component, LFA-1, has been shown to induce T-cell polarisation towards the VS to induce efficient viral T-cell-to-T-cell spread (48). In the context of VS formation between DC and T-cells it has been reported that cell-to-cell contacts are not increased by the presence of HIV-1 and the formation of the VS was

422 decreased by 60% when the interaction between ICAM-1 and LFA-1 was blocked
423 (49). Our findings agree with this data, we also observe several T-cells interacting
424 with HIV-1-infected siRNA-transfected MDDC; however accumulation of LFA-1 at the
425 VS was only evident in the presence of HIV-1 p24 Gag. These data suggest that by
426 blocking trafficking of HIV-1 to the cell periphery, enrichment of LFA-1 at the MDDC-
427 T-cell interface is also prevented, restricting VS formation. It may be the case that
428 virus alone is not the only trigger for VS formation and it is plausible that by blocking
429 trafficking of HIV-1 to the cell surface in MDDC we may also be preventing the
430 recruitment of other key components to form efficient VS.

431 We also observe the retention of endogenous CD81 in cytoplasmic vesicles
432 and a reduction of localisation at the cell periphery. In addition, at 4 hours post-
433 infection, TEMs are reduced or disrupted and potentially affecting the recruitment
434 and budding of HIV-1 at the VS. The tetraspanin CD81 co-localises with HIV-1 within
435 VCC (4, 18, 41) and accumulates at the VS promoting viral *trans*-infection, preventing
436 cell-to-cell fusion and providing a platform for viral budding (50, 51). Our results are
437 consistent with these findings suggesting that trafficking of CD81 within MDDC to
438 the plasma membrane and recruitment to TEMs, along with HIV-1, are required for
439 *trans*-infection. This is supported further by a study showing that blocking CD81 with
440 specific antibodies reduces VS formation (52). Although conversely, Krementsov and
441 colleagues show that direct depletion of CD81 actually enhances viral transmission
442 between HeLa and Jurkat cells (53). The different outcomes observed in these
443 studies may reflect the different methods and cell types employed to target CD81
444 and reduce its presence at the VS. Our data supports the former approach where
445 CD81 is still present within the cell, but is prevented from forming functioning TEMs

446 at the cell periphery, whereas actual depletion of CD81 from cells may have a
447 number of downstream effects, altering normal cell function.

448 Overall, we demonstrate that targeting host factors that regulate endocytic
449 compartments and vesicle trafficking to the plasma membrane within MDDC results
450 in the disruption of trafficking of CD81 and virus to the VS reducing *trans*-infection.

451 Our results show that upon disruption of target genes, protein trafficking to
452 lysosomes and recycling of transferrin to the plasma membrane is reduced: this
453 suggests that endosomal sorting and recycling to the plasma membrane are closely
454 linked to *trans*-infection in MDDC.

455 In conjunction with other ARF proteins, ARF1 plays an important role in the
456 regulation of recycling endosome morphology and recycling pathways, however
457 depletion of the gene was not found to directly affect the recycling of transferrin
458 receptor (54, 55). Depletion of ARF1 in our study is consistent with this role in
459 protein recycling in MDDC, altering endosomal morphology but not affecting
460 recycling of transferrin to the plasma membrane. In the context of infection, HIV-1
461 ability to mediate the down-regulation of MHC-1 is achieved by targeting AP-1 and
462 ARF1 activity (56) resulting in the accumulation of MHC-1 in the TGN or endosomes
463 (57). HIV-1 Vpu also targets the same pathway (58, 59) to counteract tetherin,
464 known to block the release of progeny virus from the cell (60). This data in
465 conjunction with the fact that ARF1 binding partner AP1M1 was originally identified
466 as a potential gene required for *trans*-infection in our screen, supports the idea that
467 the same recycling pathway could be utilised for the successful *trans*-infection of
468 HIV-1 in DC. Depletion of ARF1 is likely to impact on the morphology of virus
469 containing compartments and recycling of internalised virus to the cell surface,

which in turn reduces the accumulation of virus at the VS and therefore *trans*-infection.

BIN-1 is a key player in membrane remodelling during endocytosis and endosomal sorting, essential for the formation of plasma invaginations in muscle tissue (61). BIN-1 mutants were found to both impair membrane tabulation and cause compact membrane curvature (62). Our findings support these data: depletion of BIN-1 in MDDC reduces endosomal size, producing small round vesicles preventing downstream trafficking. A role for BIN-1 in HIV-1 infection is supported further by a study that identifies the up-regulation of BIN-1 in CD4+ and CD8+ T-cells from *ex vivo* patients (63). Based on this, we propose that BIN-1 is required for the efficient formation and function of plasma membrane invaginations and endosomal sorting that assist the trafficking of HIV-1 to the VS.

RAB7L1 is also found to have a role in intracellular trafficking and the endosomal sorting of lysosomal bound membrane proteins (64). Again, our results support a similar role for RAB7L1 in MDDC, the transport of both LDL and transferrin was impaired in RAB7L1 depleted MDDC, suggesting that trafficking from endosomal compartments is compromised. The finding that RAB7L1 along with AP1M1 are involved in HIV-1 Gag trafficking and virion budding in the activated macrophage cell line MM6 and CD4+ Jurkat cells (65), supports a role for RAB7L1 in the recruitment of HIV-1 particles in MDDC to the VS to assist viral budding at the cell surface.

RAB8A is known to control vesicular transport and promote membrane protrusions, which can be inhibited by blocking membrane recycling (66) agreeing with our findings. Knockdown of RAB8A by siRNA in previous studies was found to inhibit HIV-1 replication in Hela P4/R5 cells and directly interact with nef, env and

gag-pol (67). Therefore, it seems plausible that the depletion of RAB8A in MDDC inhibits membrane recycling and therefore membrane protrusions, reducing HIV-1 *trans*-infection. The data also supports the idea that HIV-1 taken up by MDDC could rely on the same recycling pathways to traffic to the cell membrane to accumulate virus at the VS.

The data presented in this study clearly points to a role for endocytic recycling pathways in HIV-1 *trans*-infection; therefore we investigated the retromer complex implication in the trafficking of HIV-1 to the VS. Retromer-dependent protein sorting pathways provide an opportune target for a variety of viral and bacterial pathogens (68, 69). For instance, HIV-1 envelope protein and herpesvirus saimiri, a T-lymphotrophic tumour virus, bind the retromer to aid infection and viral release (44, 70), whereas influenza A M2 protein escapes degradation via transportation from early endosomes to the TGN (71). Our data confirms a role for the retromer in DC-mediated HIV-1 *trans*-infection and exploitation of recycling pathways by the virus to achieve efficient transfer between cells.

We hypothesise that VCC and VS formation is dependent on the retromer-dependent endocytic-TGN-plasma recycling pathway. By exploiting the retromer pathway, internalised viral particles can be subverted to the plasma membrane where virus becomes sequestered to promote VS formation and enable *trans*-infection between MDDC and T-cells (Figure 8).

DC are among the most important cellular targets in early HIV-1 transmission. HIV-1 is thought to accumulate in 'viral endosomes' where the virus is able to exploit a pathway essential for the delivery of components to the immunological synapse and activation of T-cells (4). Uptake into DC using this method not only allows

efficient *trans*-infection to target CD4+ T-cells but also evades detection by the immune system (27), the importance of which was shown *in vivo* using a humanised mouse model (10, 11).

By using high-throughput siRNA screening we were able to identify *ARF1, BIN1, RAB7L1* and *RAB8A* that are essential for endosomal trafficking between the TGN and early endosomes and co-ordinated transport to the plasma membrane in a retromer-dependent manner. Thus, we identify key cellular trafficking proteins exploited by HIV-1 in DC to efficiently disseminate virus to target T-cells promoting *trans*-infection. A better understanding of the role of these proteins in viral transfer to T-cells may serve as potential candidates for targeted therapy to control the transfer of HIV-1 between DC and T-cells *in vivo.*

EXPERIMENTAL PROCEDURES

Ethics statement

Peripheral blood mononuclear cells (PMBC) were derived from buffy coats obtained from healthy blood donors, anonymously provided by the Welsh Blood Service, UK. Written informed consent for the use of buffy coats for research purposes was obtained from blood donors and the use of patient samples and procedures were approved by the local research ethics committee at Cardiff University.

Cells

Primary cells were isolated from PMBC of healthy blood donors using magnetic bead selection (Miltenyi Biotech). CD14+ monocytes were differentiated into immature

monocyte-derived dendritic cells (MDDC) with IL-4 and GM-CSF, as described previously (72, 73).

CD4+ T-cells were isolated using CD4+ magnetic beads (Miltenyi Biotech) and maintained in the presence of IL-2 and activated 4 days before use with 2 µg/mL phytohemagglutinin (PHA). SUP-T1 T-lymphoblasts and 293T human embryonic kidney (HEK) cells (obtained from NIH AIDS Research & Reference Reagent Program) were maintained in supplemented RPMI 1640 or DMEM respectively.

Viral stock production

Viral stocks were produced by transfection of HEK293T cells with calcium phosphate DNA precipitation of proviral plasmids encoding full length HIV-1 X4 and R5 provirus, pR9 and pR8BAL respectively (plasmids provided by Trono D, EPFL, Lausanne). Infectious titres were determined by titration onto SUP-T1 cells and quantification of HIV-1 p24 Gag by ELISA using the Lenti-X p24 rapid titre kit (Clontech).

Antibodies and reagents

HIV-1 p24 was detected using anti-HIV-1 core antigen antibody-FITC (KC57-FITC – Beckman Coulter), and actin labelled with Cytopainter Phallodin-iFluor-555 (abcam). Protein knockdown was detected by immunoblotting using rabbit anti-ARF1, anti-BIN1, anti-RAB8A, mouse anti-Rab7L1 (abcam), and Actin (Merck) followed by secondary HRP conjugated goat anti-rabbit and anti-mouse (DAKO). Confocal microscopy was carried out using primary antibodies, anti-human CD81-APC (BD), anti-EEA1, anti-CHMP2B, anti-LAMP1, anti-Rab7, anti-Rab11, anti-Rab5 (abcam). Horse radish peroxidase (HRP) uptake was detected using anti-HRP (Jackson

565 Immunolaboratory). All unlabelled primary antibodies were detected with secondary
566 anti-rabbit Alexa Fluor 546 (Life technologies). Pharmacological inhibitors: LY294002,
567 Bafilomycin A1, Indinivir (Sigma Aldrich) were used at 50 µM, 0.5 µM and 2 µg/mL
568 respectively.
569
570
571
572 **RNAi screen in MDDC**
573 siRNA screen was performed using a commercially available SMARTpool ON-TARGET
574 library containing 140 membrane trafficking genes (Dharmacon-GE Healthcare, also
575 see table S1). MDDC (1 x10^5 cells/well) seeded in 96 well plates were reverse
576 transfected twice, 24 hours apart, with 200 nM of pooled siRNA or with control
577 siRNA (SMARTpool ON-TARGET Non-target siRNA, Dharmacon-GE Healthcare) using
578 HiPerFect transfection reagent (Qiagen) in serum free media. After 48 hours, MDDC
579 were infected with 20-30 ng p24 Gag HIV-1 R9 by spinoculation and co-cultured with
580 SUP-T1 or CD4+ T-cells pre-stained with Celltrace™ Far Red (Invitrogen) in the
581 presence of Indinivir 2 µg/mL (Sigma) for a further 48 hours, as previously described
582 (72).
583
584 **Flow Cytometry**
585 Phenotyping of primary cells was performed by washing MDDC and CD4+ T-cells in
586 ice cold buffer (PBS, 0.5% BSA) before staining for HLR-DR, CD209, CD83 or CD14-
587 APC (BD). SUP-T1 and autologous T-cells were labelled with CD4 and CD3-APC (BD).
588 Cell viability was assessed using LIVE/DEAD stain 1:1000 (Life Technologies) in PBS,

as per manufacturer's instructions. Infected MDDC and CD4+ T-cells were fixed in 2% PFA and stained for HIV-1 p24 Gag-FITC after permeabilisation with 1x PhosFlow buffer (BD). Stained samples were washed twice before measurements were taken on the FACS Calibur (Beckton Dickinson) Canto II and analysed using Flowjo V10 software (Flowjo, LLC).

Transfer Assay

MDDC (1 x10^5 cells/well) were reverse transfected twice, 24 hours apart, with 200 nM of pooled or individual siRNA using HiPerFect transfection reagent (Qiagen) in serum free media. After 48 hours, MDDC were infected with 5-10 ng p24 Gag HIV-1 R9 or 2-5 ng p24 Gag HIV-1 R8BAL by spinoculation for 2 hours and co-cultured with CD4+ T-cells pre-stained with Celltrace™ Far red (Invitrogen) at 37°C for a further 48 hours.

Western Blot Analysis

At 72 hours post-transfection cells were lysed with 1x cell lysis buffer (Cell Signalling) and supernatants harvested and reduced. Cell lysates were separated on a 4-12% SDS-PAGE gel and run next to a PAGEruler (Thermofisher) before being subjected to western blotting followed by ECL detection and densitometry analysis (MyImage Analysis, ThermoScientific).

Uptake Assays

612 Transfected MDDC were incubated with HRP (Sigma) 10 mg/mL for 1 hour at 4°C
613 prior to fixation on coverslips using 2% Paraformaldehyde (PFA) and labelled using
614 indicated antibodies.
615 Transfected MDDC ($1x10^5$) were seeded onto poly-L-lysine coverslips and placed at
616 4°C for 10 minutes prior to the addition of either 12 µg/mL LDL-DIL (Life
617 Technologies) for 4 hours or 25 µg/mL Tranferrin Alexa Fluor 488 (Life Technologies)
618 for 30 minutes, both at 37°C. Cells were fixed in 1% PFA and nuclei labelled with
619 TOPRO-3 (Life Technologies).
620
621 **Inhibition assays**
622 Inhibitors LY294002 (50 µM) and Bafilomycin A1 (0.5 µM) were added to MDDC 1
623 hour prior to and during infection with R9 HIV-1. DMSO was used as a control at
624 equal concentrations. Cells were either seeded on coverslips and fixed in 2% PFA for
625 confocal imaging, or washed and co-cultured with CD4+ T-cells for 48 hours at 37°C
626 for analysis via flow cytometry.
627
628 **Virological synapse assay**
629 MDDC transfected with siRNA were infected with HIV-1 for 2 hours prior to
630 incubation with CD4+ T-cells on Poly-L-Lysine coverslips at 1:1 ratio for 40 minutes at
631 37°C. Fixed cells (2% PFA) were labelled for Actin and p24 Gag-FITC and viewed on
632 the confocal microscope. Virological synapse formation was counted if an
633 accumulation (approx. 50% or greater) of p24 Gag was evident at or adjacent to the
634 junction between T-cells and MDDC. T-cells were identified by their smaller size and
635 less cytoplasmic content in comparison to larger MDDC.

636

637 **Confocal Immunofluorescence**

638 Cells were adhered to Poly-L-Lysine coverslips (Corning), fixed in 2% PFA,
639 permeabilised with 0.05% saponin and stained with indicated primary antibodies in
640 PBS/0.2% BSA/0.05% saponin followed by Alexa Fluor labelled secondary antibodies
641 (1:400) when necessary. TOPRO3 in PBS (1:1000) was used to stain nuclei (Life
642 Technologies). Confocal microscopy analysis was carried out using Zeiss LSM710
643 using 100x oil objective with 488, 546, 633nm acquired sequentially using ZENlite
644 software (Zeiss). All confocal images represent a single plane. Co-localisation analysis
645 was performed using Zenlite software (Zen Blue) using the co-localisation function.

646

647 **Bioinformatics - Protein Interrelationship mapping**

648 RNAi screen candidates were enriched using DAVID to identify significant gene
649 ontology (GO) terms and a protein-protein interaction network was visualised using
650 EnrichmentMap (Bader Lab) plug-in for Cytoscape 3.3.3; the top 5 significant values
651 were reported. The minimum confidence score was set at 0.005 (74-77).

652

653 **Image Analysis**

654 Image analysis was performed using ImageJ software (NIH) and analysed with Excel
655 software (Microsoft). A macro was designed to apply a set scale to all images
656 followed by the colour threshold to eliminate any background staining and the
657 particle analysis function was applied to quantify vesicles. Pixels were converted to
658 µM using the set scale.

659

Statistics

Data was analysed using a two-sample T-Test, comparing non-target to targeted siRNA samples. A one sample T-test was used to compare siRNA transfer assays across donors. P-values <0.05, <0.005, <0.0005 were considered significant marked *, **and *** respectively. Data was analysed using Prism (Graphpad) software.

ACKNOWLEDGMENTS

We thank Dr. Svetlana Hakobyan for laboratory support. This work was funded by The Wellcome Trust seedcorn award, Cardiff University and The Bill and Melinda Gate foundation awarded to VP, as well as DFG SFB 829 A1&A5 to CMN.

AUTHOR CONTRIBUTIONS

Conceptualization, V.P. and R.B. Methodology, R.B., V.P., C.M.N. and S.C. Investigation and validation, R.B. Formal Analysis, R.B. and J.W. Writing –original draft and visualisation, R.B. Writing – review and editing, S.C., V.P. and C.M.N. Funding acquisition and supervision, V.P.

REFERENCES

1. **Piguet V, Steinman RM.** 2007. The interaction of HIV with dendritic cells: outcomes and pathways. Trends Immunol **28:**503-510.

2. **Law KM, Satija N, Esposito AM, Chen BK.** 2016. Cell-to-Cell Spread of HIV and Viral Pathogenesis. Adv Virus Res **95:**43-85.

3. **Turville SG, Santos JJ, Frank I, Cameron PU, Wilkinson J, Miranda-Saksena M, Dable J, Stossel H, Romani N, Piatak M, Jr., Lifson JD, Pope M, Cunningham AL.** 2004. Immunodeficiency virus uptake, turnover, and 2-phase transfer in human dendritic cells. Blood **103:**2170-2179.

4. **Garcia E, Pion M, Pelchen-Matthews A, Collinson L, Arrighi JF, Blot G, Leuba F, Escola JM, Demaurex N, Marsh M, Piguet V.** 2005. HIV-1 trafficking to the dendritic cell-T-cell infectious synapse uses a pathway of tetraspanin sorting to the immunological synapse. Traffic **6:**488-501.

5. **Nobile C, Petit C, Moris A, Skrabal K, Abastado JP, Mammano F, Schwartz O.** 2005. Covert human immunodeficiency virus replication in dendritic cells and in DC-SIGN-expressing cells promotes long-term transmission to lymphocytes. J Virol **79:**5386-5399.

6. **Moris A, Pajot A, Blanchet F, Guivel-Benhassine F, Salcedo M, Schwartz O.** 2006. Dendritic cells and HIV-specific CD4+ T cells: HIV antigen presentation, T-cell activation, and viral transfer. Blood **108:**1643-1651.

7. **Wang JH, Janas AM, Olson WJ, Wu L.** 2007. Functionally distinct transmission of human immunodeficiency virus type 1 mediated by immature and mature dendritic cells. J Virol **81:**8933-8943.

8. **Wu L, KewalRamani VN.** 2006. Dendritic-cell interactions with HIV: infection and viral dissemination. Nat Rev Immunol **6:**859-868.

9. **Geijtenbeek TB, Kwon DS, Torensma R, van Vliet SJ, van Duijnhoven GC, Middel J, Cornelissen IL, Nottet HS, KewalRamani VN, Littman DR, Figdor CG, van Kooyk Y.** 2000. DC-SIGN, a dendritic cell-specific HIV-1-binding protein that enhances trans-infection of T cells. Cell **100:**587-597.

10. **Sewald X, Ladinsky MS, Uchil PD, Beloor J, Pi R, Herrmann C, Motamedi N, Murooka TT, Brehm MA, Greiner DL, Shultz LD, Mempel TR, Bjorkman PJ, Kumar P, Mothes W.** 2015. Retroviruses use CD169-mediated trans-infection of permissive lymphocytes to establish infection. Science **350:**563-567.

11. **Law KM, Komarova NL, Yewdall AW, Lee RK, Herrera OL, Wodarz D, Chen BK.** 2016. In Vivo HIV-1 Cell-to-Cell Transmission Promotes Multicopy Micro-compartmentalized Infection. Cell Rep **15:**2771-2783.

12. **Cavrois M, Neidleman J, Kreisberg JF, Greene WC.** 2007. In vitro derived dendritic cells trans-infect CD4 T cells primarily with surface-bound HIV-1 virions. PLoS Pathog **3:**e4.

13. **Menager MM, Littman DR.** 2016. Actin Dynamics Regulates Dendritic Cell-Mediated Transfer of HIV-1 to T Cells. Cell **164:**695-709.

14. **Izquierdo-Useros N, Lorizate M, Puertas MC, Rodriguez-Plata MT, Zangger N, Erikson E, Pino M, Erkizia I, Glass B, Clotet B, Keppler OT, Telenti A, Krausslich HG, Martinez-Picado J.** 2012. Siglec-1 is a novel dendritic cell receptor that mediates HIV-1 trans-infection through recognition of viral membrane gangliosides. PLoS Biol **10:**e1001448.

15. **Yu HJ, Reuter MA, McDonald D.** 2008. HIV traffics through a specialized, surface-accessible intracellular compartment during trans-infection of T cells by mature dendritic cells. PLoS Pathog **4:**e1000134.

16. **Chu H, Wang JJ, Qi M, Yoon JJ, Wen X, Chen X, Ding L, Spearman P.** 2012. The intracellular virus-containing compartments in primary human macrophages are largely inaccessible to antibodies and small molecules. PLoS One **7:**e35297.

17. **Mlcochova P, Pelchen-Matthews A, Marsh M.** 2013. Organization and regulation of intracellular plasma membrane-connected HIV-1 assembly compartments in macrophages. BMC Biol **11:**89.

18. **Garcia E, Nikolic DS, Piguet V.** 2008. HIV-1 replication in dendritic cells occurs through a tetraspanin-containing compartment enriched in AP-3. Traffic **9:**200-214.

19. **Berger A, Sommer AF, Zwarg J, Hamdorf M, Welzel K, Esly N, Panitz S, Reuter A, Ramos I, Jatiani A, Mulder LC, Fernandez-Sesma A, Rutsch F, Simon V, Konig R, Flory E.** 2011. SAMHD1-deficient CD14+ cells from individuals with Aicardi-Goutieres syndrome are highly susceptible to HIV-1 infection. PLoS Pathog **7:**e1002425.

20. **Hrecka K, Hao C, Gierszewska M, Swanson SK, Kesik-Brodacka M, Srivastava S, Florens L, Washburn MP, Skowronski J.** 2011. Vpx relieves inhibition of HIV-1 infection of macrophages mediated by the SAMHD1 protein. Nature **474:**658-661.

21. **Goldstone DC, Ennis-Adeniran V, Hedden JJ, Groom HC, Rice GI, Christodoulou E, Walker PA, Kelly G, Haire LF, Yap MW, de Carvalho LP, Stoye JP, Crow YJ, Taylor IA, Webb M.** 2011. HIV-1 restriction factor SAMHD1 is a deoxynucleoside triphosphate triphosphohydrolase. Nature **480:**379-382.

22. **Lahouassa H, Daddacha W, Hofmann H, Ayinde D, Logue EC, Dragin L, Bloch N, Maudet C, Bertrand M, Gramberg T, Pancino G, Priet S, Canard B, Laguette N, Benkirane M, Transy C, Landau NR, Kim B, Margottin-Goguet F.** 2012. SAMHD1 restricts the replication of human immunodeficiency virus type 1 by depleting the intracellular pool of deoxynucleoside triphosphates. Nat Immunol **13:**223-228.

23. **Laguette N, Sobhian B, Casartelli N, Ringeard M, Chable-Bessia C, Segeral E, Yatim A, Emiliani S, Schwartz O, Benkirane M.** 2011. SAMHD1 is the dendritic- and myeloid-cell-specific HIV-1 restriction factor counteracted by Vpx. Nature **474:**654-657.

24. **Reinhard C, Bottinelli D, Kim B, Luban J.** 2014. Vpx rescue of HIV-1 from the antiviral state in mature dendritic cells is independent of the intracellular deoxynucleotide concentration. Retrovirology **11:**12.

25. **Gao D, Wu J, Wu YT, Du F, Aroh C, Yan N, Sun L, Chen ZJ.** 2013. Cyclic GMP-AMP synthase is an innate immune sensor of HIV and other retroviruses. Science **341:**903-906.

26. **Lahaye X, Satoh T, Gentili M, Cerboni S, Conrad C, Hurbain I, El Marjou A, Lacabaratz C, Lelievre JD, Manel N.** 2013. The capsids of HIV-1 and HIV-2 determine immune detection of the viral cDNA by the innate sensor cGAS in dendritic cells. Immunity **39:**1132-1142.

27. **Manel N, Hogstad B, Wang Y, Levy DE, Unutmaz D, Littman DR.** 2010. A cryptic sensor for HIV-1 activates antiviral innate immunity in dendritic cells. Nature **467:**214-217.

28. **Frank I, Piatak M, Jr., Stoessel H, Romani N, Bonnyay D, Lifson JD, Pope M.** 2002. Infectious and whole inactivated simian immunodeficiency viruses interact similarly with primate dendritic cells (DCs): differential intracellular fate of virions in mature and immature DCs. J Virol **76:**2936-2951.

29. **Wong AW, Scales SJ, Reilly DE.** 2007. DNA internalized via caveolae requires microtubule-dependent, Rab7-independent transport to the late endocytic pathway for delivery to the nucleus. J Biol Chem **282:**22953-22963.

30. **de Witte L, Nabatov A, Pion M, Fluitsma D, de Jong MA, de Gruijl T, Piguet V, van Kooyk Y, Geijtenbeek TB.** 2007. Langerin is a natural barrier to HIV-1 transmission by Langerhans cells. Nat Med **13:**367-371.

31. **Kwon DS, Gregorio G, Bitton N, Hendrickson WA, Littman DR.** 2002. DC-SIGN-mediated internalization of HIV is required for trans-enhancement of T cell infection. Immunity **16:**135-144.

32. **Wang JH, Wells C, Wu L.** 2008. Macropinocytosis and cytoskeleton contribute to dendritic cell-mediated HIV-1 transmission to CD4+ T cells. Virology **381:**143-154.

33. **Hammonds JE, Beeman N, Ding L, Takushi S, Francis AC, Wang JJ, Melikyan GB, Spearman P.** 2017. Siglec-1 initiates formation of the virus-containing compartment and enhances macrophage-to-T cell transmission of HIV-1. PLoS Pathog **13:**e1006181.

34. **Aniento F, Gu F, Parton RG, Gruenberg J.** 1996. An endosomal beta COP is involved in the pH-dependent formation of transport vesicles destined for late endosomes. J Cell Biol **133:**29-41.

35. **Gu F, Gruenberg J.** 2000. ARF1 regulates pH-dependent COP functions in the early endocytic pathway. J Biol Chem **275:**8154-8160.

36. **Meinecke M, Boucrot E, Camdere G, Hon WC, Mittal R, McMahon HT.** 2013. Cooperative recruitment of dynamin and BIN/amphiphysin/Rvs (BAR) domain-containing proteins leads to GTP-dependent membrane scission. J Biol Chem **288:**6651-6661.

37. **MacLeod DA, Rhinn H, Kuwahara T, Zolin A, Di Paolo G, McCabe BD, Marder KS, Honig LS, Clark LN, Small SA, Abeliovich A.** 2013. RAB7L1 interacts with LRRK2 to modify intraneuronal protein sorting and Parkinson's disease risk. Neuron **77:**425-439.

38. **Peranen J, Auvinen P, Virta H, Wepf R, Simons K.** 1996. Rab8 promotes polarized membrane transport through reorganization of actin and microtubules in fibroblasts. J Cell Biol **135:**153-167.

39. **McDonald D, Wu L, Bohks SM, KewalRamani VN, Unutmaz D, Hope TJ.** 2003. Recruitment of HIV and its receptors to dendritic cell-T cell junctions. Science **300:**1295-1297.

40. **Arrighi JF, Pion M, Garcia E, Escola JM, van Kooyk Y, Geijtenbeek TB, Piguet V.** 2004. DC-SIGN-mediated infectious synapse formation enhances X4 HIV-1 transmission from dendritic cells to T cells. J Exp Med **200:**1279-1288.

41. **Deneka M, Pelchen-Matthews A, Byland R, Ruiz-Mateos E, Marsh M.** 2007. In macrophages, HIV-1 assembles into an intracellular plasma membrane domain containing the tetraspanins CD81, CD9, and CD53. J Cell Biol **177:**329-341.

42. **Dale BM, Alvarez RA, Chen BK.** 2013. Mechanisms of enhanced HIV spread through T-cell virological synapses. Immunol Rev **251:**113-124.

43. **Chen C, Garcia-Santos D, Ishikawa Y, Seguin A, Li L, Fegan KH, Hildick-Smith GJ, Shah DI, Cooney JD, Chen W, King MJ, Yien YY, Schultz IJ, Anderson H, Dalton AJ, Freedman ML, Kingsley PD, Palis J, Hattangadi SM, Lodish HF, Ward DM, Kaplan J, Maeda T, Ponka P, Paw BH.** 2013. Snx3 regulates recycling of the transferrin receptor and iron assimilation. Cell Metab **17:**343-352.

44. **Groppelli E, Len AC, Granger LA, Jolly C.** 2014. Retromer regulates HIV-1 envelope glycoprotein trafficking and incorporation into virions. PLoS Pathog **10:**e1004518.

45. **Wen X, Ding L, Hunter E, Spearman P.** 2014. An siRNA screen of membrane trafficking genes highlights pathways common to HIV-1 and M-PMV virus assembly and release. PLoS One **9:**e106151.

46. **Menager MM.** 2017. TSPAN7, effector of actin nucleation required for dendritic cell-mediated transfer of HIV-1 to T cells. Biochem Soc Trans **45:**703-708.

47. **Wang L, Eng ET, Law K, Gordon RE, Rice WJ, Chen BK.** 2017. Visualization of HIV T Cell Virological Synapses and Virus-Containing Compartments by Three-Dimensional Correlative Light and Electron Microscopy. J Virol **91**.

48. **Starling S, Jolly C.** 2016. LFA-1 Engagement Triggers T Cell Polarization at the HIV-1 Virological Synapse. J Virol **90:**9841-9854.

847 49. **Rodriguez-Plata MT, Puigdomenech I, Izquierdo-Useros N, Puertas MC, Carrillo J, Erkizia I, Clotet B, Blanco J, Martinez-Picado J.** 2013. The infectious synapse formed between mature dendritic cells and CD4(+) T cells is independent of the presence of the HIV-1 envelope glycoprotein. Retrovirology **10:**42.

852 50. **Weng J, Krementsov DN, Khurana S, Roy NH, Thali M.** 2009. Formation of syncytia is repressed by tetraspanins in human immunodeficiency virus type 1-producing cells. J Virol **83:**7467-7474.

855 51. **Jolly C, Sattentau QJ.** 2007. Human immunodeficiency virus type 1 assembly, budding, and cell-cell spread in T cells take place in tetraspanin-enriched plasma membrane domains. J Virol **81:**7873-7884.

858 52. **Grigorov B, Attuil-Audenis V, Perugi F, Nedelec M, Watson S, Pique C, Darlix JL, Conjeaud H, Muriaux D.** 2009. A role for CD81 on the late steps of HIV-1 replication in a chronically infected T cell line. Retrovirology **6:**28.

861 53. **Krementsov DN, Weng J, Lambele M, Roy NH, Thali M.** 2009. Tetraspanins regulate cell-to-cell transmission of HIV-1. Retrovirology **6:**64.

863 54. **Kondo Y, Hanai A, Nakai W, Katoh Y, Nakayama K, Shin HW.** 2012. ARF1 and ARF3 are required for the integrity of recycling endosomes and the recycling pathway. Cell Struct Funct **37:**141-154.

866 55. **Nakai W, Kondo Y, Saitoh A, Naito T, Nakayama K, Shin HW.** 2013. ARF1 and ARF4 regulate recycling endosomal morphology and retrograde transport from endosomes to the Golgi apparatus. Mol Biol Cell **24:**2570-2581.

870 56. **Coleman SH, Hitchin D, Noviello CM, Guatelli JC.** 2006. HIV-1 Nef stabilizes AP-1 on membranes without inducing ARF1-independent de novo attachment. Virology **345:**148-155.

873 57. **Lubben NB, Sahlender DA, Motley AM, Lehner PJ, Benaroch P, Robinson MS.** 2007. HIV-1 Nef-induced down-regulation of MHC class I requires AP-1 and clathrin but not PACS-1 and is impeded by AP-2. Mol Biol Cell **18:**3351-3365.

877 58. **Kueck T, Foster TL, Weinelt J, Sumner JC, Pickering S, Neil SJ.** 2015. Serine Phosphorylation of HIV-1 Vpu and Its Binding to Tetherin Regulates Interaction with Clathrin Adaptors. PLoS Pathog **11:**e1005141.

880 59. **Schmidt S, Fritz JV, Bitzegeio J, Fackler OT, Keppler OT.** 2011. HIV-1 Vpu blocks recycling and biosynthetic transport of the intrinsic immunity factor CD317/tetherin to overcome the virion release restriction. MBio **2:**e00036-00011.

884 60. **Sauter D, Schindler M, Specht A, Landford WN, Munch J, Kim KA, Votteler J, Schubert U, Bibollet-Ruche F, Keele BF, Takehisa J, Ogando Y, Ochsenbauer C, Kappes JC, Ayouba A, Peeters M, Learn GH, Shaw G, Sharp PM, Bieniasz P, Hahn BH, Hatziioannou T, Kirchhoff F.** 2009.

Tetherin-driven adaptation of Vpu and Nef function and the evolution of pandemic and nonpandemic HIV-1 strains. Cell Host Microbe **6:**409-421.

61. **Tjondrokoesoemo A, Park KH, Ferrante C, Komazaki S, Lesniak S, Brotto M, Ko JK, Zhou J, Weisleder N, Ma J.** 2011. Disrupted membrane structure and intracellular Ca(2)(+) signaling in adult skeletal muscle with acute knockdown of Bin1. PLoS One **6:**e25740.

62. **Wu T, Shi Z, Baumgart T.** 2014. Mutations in BIN1 associated with centronuclear myopathy disrupt membrane remodeling by affecting protein density and oligomerization. PLoS One **9:**e93060.

63. **Hyrcza MD, Kovacs C, Loutfy M, Halpenny R, Heisler L, Yang S, Wilkins O, Ostrowski M, Der SD.** 2007. Distinct transcriptional profiles in ex vivo CD4+ and CD8+ T cells are established early in human immunodeficiency virus type 1 infection and are characterized by a chronic interferon response as well as extensive transcriptional changes in CD8+ T cells. J Virol **81:**3477-3486.

64. **Kuwahara T, Inoue K, D'Agati VD, Fujimoto T, Eguchi T, Saha S, Wolozin B, Iwatsubo T, Abeliovich A.** 2016. LRRK2 and RAB7L1 coordinately regulate axonal morphology and lysosome integrity in diverse cellular contexts. Sci Rep **6:**29945.

65. **Yu W, Ramakrishnan R, Wang Y, Chiang K, Sung TL, Rice AP.** 2008. Cyclin T1-dependent genes in activated CD4 T and macrophage cell lines appear enriched in HIV-1 co-factors. PLoS One **3:**e3146.

66. **Zhu S, Bhat S, Syan S, Kuchitsu Y, Fukuda M, Zurzolo C.** 2018. Rab11a-Rab8a cascade regulates the formation of tunneling nanotubes through vesicle recycling. J Cell Sci **131**.

67. **Zhou H, Xu M, Huang Q, Gates AT, Zhang XD, Castle JC, Stec E, Ferrer M, Strulovici B, Hazuda DJ, Espeseth AS.** 2008. Genome-scale RNAi screen for host factors required for HIV replication. Cell Host Microbe **4:**495-504.

68. **Abubakar YS, Zheng W, Olsson S, Zhou J.** 2017. Updated Insight into the Physiological and Pathological Roles of the Retromer Complex. Int J Mol Sci **18**.

69. **Wang J, Fedoseienko A, Chen B, Burstein E, Jia D, Billadeau DD.** 2018. Endosomal receptor trafficking: Retromer and beyond. Traffic **19:**578-590.

70. **Kingston D, Chang H, Ensser A, Lee HR, Lee J, Lee SH, Jung JU, Cho NH.** 2011. Inhibition of retromer activity by herpesvirus saimiri tip leads to CD4 downregulation and efficient T cell transformation. J Virol **85:**10627-10638.

71. **Bhowmick S, Chakravarty C, Sellathamby S, Lal SK.** 2017. The influenza A virus matrix protein 2 undergoes retrograde transport from the endoplasmic

928 reticulum into the cytoplasm and bypasses cytoplasmic proteasomal
929 degradation. Arch Virol **162:**919-929.

930 72. **Blanchet FP, Piguet V.** 2010. Immunoamphisomes in dendritic cells amplify
931 TLR signaling and enhance exogenous antigen presentation on MHC-II.
932 Autophagy **6:**816-818.

933 73. **Blanchet FP, Stalder R, Czubala M, Lehmann M, Rio L, Mangeat B,**
934 **Piguet V.** 2013. TLR-4 engagement of dendritic cells confers a BST-
935 2/tetherin-mediated restriction of HIV-1 infection to CD4+ T cells across the
936 virological synapse. Retrovirology **10:**6.

937 74. **Huang da W, Sherman BT, Lempicki RA.** 2009. Systematic and integrative
938 analysis of large gene lists using DAVID bioinformatics resources. Nat Protoc
939 **4:**44-57.

940 75. **Huang da W, Sherman BT, Lempicki RA.** 2009. Bioinformatics enrichment
941 tools: paths toward the comprehensive functional analysis of large gene lists.
942 Nucleic Acids Res **37:**1-13.

943 76. **Merico D, Isserlin R, Stueker O, Emili A, Bader GD.** 2010. Enrichment
944 map: a network-based method for gene-set enrichment visualization and
945 interpretation. PLoS One **5:**e13984.

946 77. **Shannon P, Markiel A, Ozier O, Baliga NS, Wang JT, Ramage D, Amin**
947 **N, Schwikowski B, Ideker T.** 2003. Cytoscape: a software environment for
948 integrated models of biomolecular interaction networks. Genome Res
949 **13:**2498-2504.
950

951 ## FIGURE LEGENDS

952 **Figure 1. The procedure and results of the siRNA screen used to investigate *trans*-infection**
953 **of HIV-1 between MDDC and T-cells.**

954 A) Schematic of the method used to study the effects of siRNA knockdown on HIV-1
955 trans-infection between DC and CD4+ T cells.

956 B) Results of siRNA screen on HIV-1 trans-infection between MDDC and CD4+ T-
957 cells. Red dashed lines indicate the assay cut off of -20% and +50% for non-
958 specific variation of the assay. siRNA that reduced or increased HIV-1 trans-
959 infection above or below the cut-off point (HITS) are listed in the grey boxes.

960 C) Identification of genes that reduced HIV-1 *trans*-infection between MDDC and T-
961 cells. Results from initial screen conducted in SUPT1 cells (○) are shown in

combination with repeats conducted in with autologous CD4+ T-cells (●). Mean and SD of three independent donors shown. Only genes with a mean percentage below that of the non-target siRNA are shown.

D) Identification of genes that increase HIV-1 *trans*-infection between MDDC and T-cells. Results from initial screen conducted in SUPT1 (○) cells are shown in combination with two repeats conducted in with autologous CD4+ T-cells (●). The mean and SD of three independent donors was calculated per gene. Only genes with a mean above that of the non-target siRNA are shown.

Figure 2. ARF1, BIN1, Rab7L1 and RAB8A regulate DC T-cell HIV *trans*-infection

A) Validation of siRNA knockdown on *trans*-infection against four individual siRNA from each candidate gene. Percentage of HIV-1 transfer is normalised to non-target siRNA set at a value of 1.0. Each point represents an individual donor. The mean and SD ± is shown. * p< 0.05, ** p< 0.005.

B) Western blot analysis of pooled siRNA knockdown in MDDC at 72 hours post-transfection with *ARF1, BIN1, RAB7L1* and *RAB8A* siRNA performed in triplicate, untreated MDDC and non-target siRNA. Actin is used as a loading control.

C) Densitometry quantification of protein expression levels for ARF1, BIN1, RAB7L1 and RAB8A. Protein expression levels for siRNA transfected MDDC normalised to actin loading control. All values are relative to non-target siRNA transfected lanes (Set at 1.0). Mean and SD ± shown, n=3.

D) The effects of final target siRNA on HIV-1 trans-infection infected with CXCR4 (R9). The reduction in viral transfer is measured relative to Non-target siRNA. Mean and SD shown for each sample (n = 5) * p < 0.05, ** p < 0.005.

E) The effects of final target siRNA on HIV-1 trans-infection infected with CCR5 (R8Bal). The reduction in viral transfer is measured relative to Non-target siRNA. Mean and SD shown for each sample (n = 5) * $p < 0.05$, ** $p < 0.005$.

F) The effects of ARF1, BIN1, RAB7L1, RAB8A siRNA transfection on the viability of MDDC at 48 hours post-transfection. All samples compared to untreated MDDC. Cell viability is shown as a percentage. Mean ± SD, n = 2.

Figure 3. ARF1, BIN1, RAB7L1 and RAB8A are regulators virological synapse formation between HIV-1 infected MDDC and CD4+T-cells.

A) Images of CXCR4 HIV-1 R9 (p24 green) infected, siRNA transfected MDDC interacting with CD4+ T-cells (identified with *). Actin = red, nuclei = blue. Scale= 10 µM.

B) Quantification of virological synapse formation between MDDC and CD4+ T-cells was counted in siRNA transfected MDDC infected with HIV-1 R9 and co-cultured with autologous CD4+ T-cells. T-cells were identified as the smaller cells with less cytoplasmic content compared to the larger MDDC in co-culture. Data normalised to MDDC transfected with non-target siRNA. The mean and SD of three independent donors (n = 500 cells) is shown. ** $p < 0.05$. ** $p < 0.05$.

C) Images of CCR5 HIV-1 R8BAL (p24 green) infected, siRNA transfected MDDC interacting with CD4+ T-cells (identified with *). Actin = red, nuclei = blue. Scale= 10 µM.

D) Quantification of virological synapse formation between MDDC and CD4+ T-cells was counted in transfected MDDC infected with HIV-1 R8BAL and co-cultured with autologous CD4+ T-cells. Data normalised to MDDC transfected with non-target siRNA. The mean and SD of three independent donors (n = 300 cells) is shown. ** $p < 0.05$. ** $p < 0.05$.

Figure 4. CD81 localisation and TEM formation is disrupted in MDDC transfected with ARF1, BIN1, RAB7L1 and RAB8A siRNA.

A) The effects of target siRNA on CD81 staining and localisation in MDDC. CD81= green, nuclei = blue. Scale = 10 µM.

B) Quantification of CD81 vesicles in target siRNA transfected MDDC compared to non-target siRNA control (n = 110 cells, across three independent donors). Mean and SEM shown* $p < 0.05$, *** $p < 0.0005$.

C) Average size (µM) of CD81 positive vesicles in MDDC transfected with target siRNA compared to non-target siRNA (n = 150 cells, across three independent donors). Mean and SEM shown. ** $p < 0.005$, *** $p < 0.0005$.

D) Images of CD81 (red) and HIV-1 p24 Gag (green) in infected MDDC transfected with non-target and target siRNA. Images show HIV-1 4 hours post-infection. Nuclei = Red (spherical). Scale 10 µM.

E) Quantification of CD81 and p24 at tetraspanin enriched domains (TEM) in infected MDDC at 4 hours post-infection. The mean percentage of cells with HIV-1 p24 Gag localised at CD81 enriched TEMs is represented by black bars. White bars represent the absence of CD81 enriched TEMs. Mean percentage and SD is shown. N = 170 cells, across 2 independent donors.

F) Co-localisation analysis of TEM in siRNA transfected MDDC compared to control cells. The co-localisation coefficient of CD81 with HIV-1 p24 Gag is shown for each condition. Mean and SEM± shown, n=11 fields analysed over 2 independent donors. **$p < 0.005$, *** $p < 0.0005$

Figure 5. Retention of virus in endocytic derived compartments reduces HIV trans-infection from DC to T-cells.

A) The effect of LY294002 and Bafilomycin A1 treatment on HIV-1 transfer. MDDC were pre-treated with inhibitors overnight prior to infection with HIV-1 (R9) before co-culture with autologous CD4+ T-cells for 48 hours in triplicate in 2 independent donors. Mean percentage (%) viral transfer and SD shown, ***p < 0.0005.

B) Percentage viability of MDDC after overnight incubation with LY294002 and Bafilomycin A1 at 0, 2 and 48 hours post-infection (pi). The percentage (%) of reduction in cell viability was assessed using a Live/Dead stain and analysed by flow cytometry. Mean and SD shown. Experiments performed in triplicate in 2 independent donors

The effect of inhibitor LY294002 and Bafilomycin A1 on HIV-1 localisation in MDDC. MDDC pre-treated with inhibitors were infected with HIV-1 for analysis by confocal microscopy. Labelling of p24 Gag HIV-1 = green, nuclei = blue. Scale = 10 µM.

C) The effect of LY294002 and Bafilomycin A1 on LDL-DIL and HRP uptake into MDDC. Inhibitors added overnight before the addition of LDL-DIL = green, and HRP = red, nuclei blue. Scale = 10 µM.

Figure 6. Endocytic trafficking is compromised in BIN1, RAB7L1 and RAB8A transfected MDDC.

The effect of target siRNA on vesicle trafficking in MDDC.

A) MDDC transfected with ARF1, BIN-1, Rab7L1 and RAB8A siRNA for 48 hours were either labelled with either EEA1 for early endosomes (red, panel 1), or incubated with Transferrin (green, panel 2), for 20 minutes 37°C or LDL-DIL (green, panel 3) for 2 hours 37°C. Non-target siRNA was used a control. Nuclei in Blue. Scale = 10 µM.

B) Quantification of EEA1 vesicles in MDDC transfected with target siRNA compared to non-target siRNA control (n = 150 cells). Mean and SEM from three independent donors shown, * $p < 0.05$, *** $p < 0.0005$.

C) Average EEA1 vesicle size (µM) in MDDC transfected with target siRNA compared to non-target siRNA control (n = 150 cells). Mean and SEM from three independent donors shown, *** $p < 0.0005$.

D) Quantification of the number of transferrin positive vesicles under each condition compared to non-target control (n=150). Mean and SEM from three independent donors shown. *$p < 0.05$.

E) Measurement of the intensity of Transferrin in transfected MDDC under each condition compared to non-target control (n=150). Mean and SEM from three independent donors shown. *$p < 0.05$, **$p < 0.005$.

F) Quantitative analysis of LDL-DIL containing vesicles (n = 120). Mean and SEM from three independent donors shown, * $p < 0.05$, *** $p < 0.0005$.

G) Intensity of LDL-DIL in transfected MDDC compared to non-target siRNA (n = 120). Mean and SEM from three independent donors shown, * $p < 0.05$.

Figure 7. HIV-1 trans-infection requires retromer recycling to the plasma membrane.

A-B) The reduction in HIV-1 trans-infection between MDDC and CD4+ T-cells in MDDC transfected with VPS26A and VPS35 via siRNA transfection. The reduction in trans-infection is normalised to non-target siRNA for R9 (d) and R8-BAL (e). Mean ± SD is shown, n = 4. *$p < 0.05$, ***$p < 0.0001$.

C-D) Western blots showing the knockdown of VPS26A and VPS35 in MDDC, performed in triplicate, compared to untreated cell lysate and non-target siRNA transfected MDDC. Actin used as a loading control.

E) Quantification of protein knockdown of VPS26A and VPS35 in transfected MDDC relative to non-target lane. All lanes compared to corresponding Actin loading control (black bars). Mean and ± SD shown, n = 3.

Figure 8 Model for the roles of ARF1, BIN1, RAB7L1 and RAB8A in the endocytic pathway and vesicle formation in MDDC.

Molecules are internalised from the cell surface via endocytic vesicles that fuse with each other or existing endocytic vesicles to form early endosomes. The budding of vesicles containing cargo from early endosomes to the plasma membrane and trans-Golgi network (TGN) requires the activity of BIN1. TGN vesicles bud from the TGN surface and either fuse with each other or endocytic compartments. The TGN is responsible for sorting receptors from degradative compartments and delivers newly synthesised lysosomal enzymes in the form of lysosomal hydrolase via the mannose-6-phosphate receptor. Both transferrin and LDL are taken into the cell via clathrin-receptor mediated endocytosis. Transferrin and its receptor are recycled from early endosomes back to the plasma membrane. LDL is trafficked directly to lysosomes prior to release into the cytoplasm. The dynamic retrograde transport of vesicles between the TGN and endocytic compartment and the plasma membrane via the retromer and other trafficking pathways required depends on the activity of ARF1, RAB7L1 and RAB8A. HIV-1 *trans*-infection between MDDC and CD4+ T-cells requires a homeostatic balance of the endocytic pathway. By blocking trafficking of molecules between early endosomes and the TGN and onward polarised transport of cargo to the plasma membrane, HIV-1 trans-infection is inhibited. Depletion of targeted proteins results in the accumulation of HIV-1 in intracellular vesicles that are unable to traffic to the virological synapse

Table 1

Network analysis statistical data

A) Statistical Data (p- and q-values) for biological processes of genes inhibitory to HIV-1 *trans*-infection. Values < 0.005 are displayed for each node name. The number of data sets included in the process are indicated under the dataset size heading.

B) Statistical Data (p- and q-values) for biological processes of genes facilitating HIV-1 *trans*-infection. Values < 0.005 are displayed for each node name. The number of data sets included in the process are indicated under the dataset size heading

C) Statistical Data (p- and q-values) for cellular compartments of genes inhibitory to HIV-1 *trans*-infection. Values < 0.005 are displayed for each node name. The numbers of data sets associated with the cellular compartments are indicated under the dataset size heading.

D) Statistical Data (p- and q-values) for cellular compartments of genes facilitating HIV-1 *trans*-infection. Values < 0.005 are displayed for each node name. The numbers of data sets included in the process are indicated under the dataset size heading.

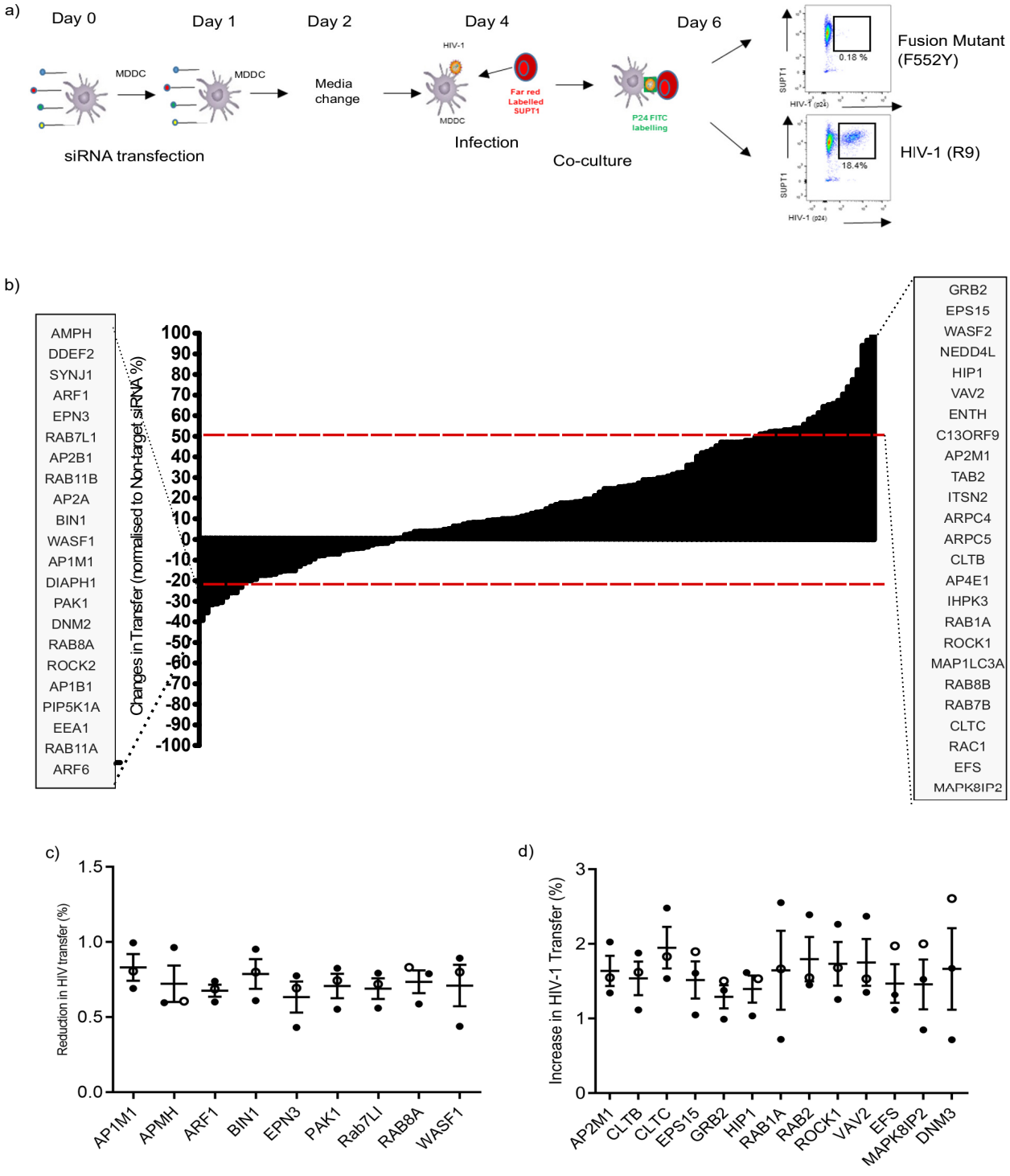

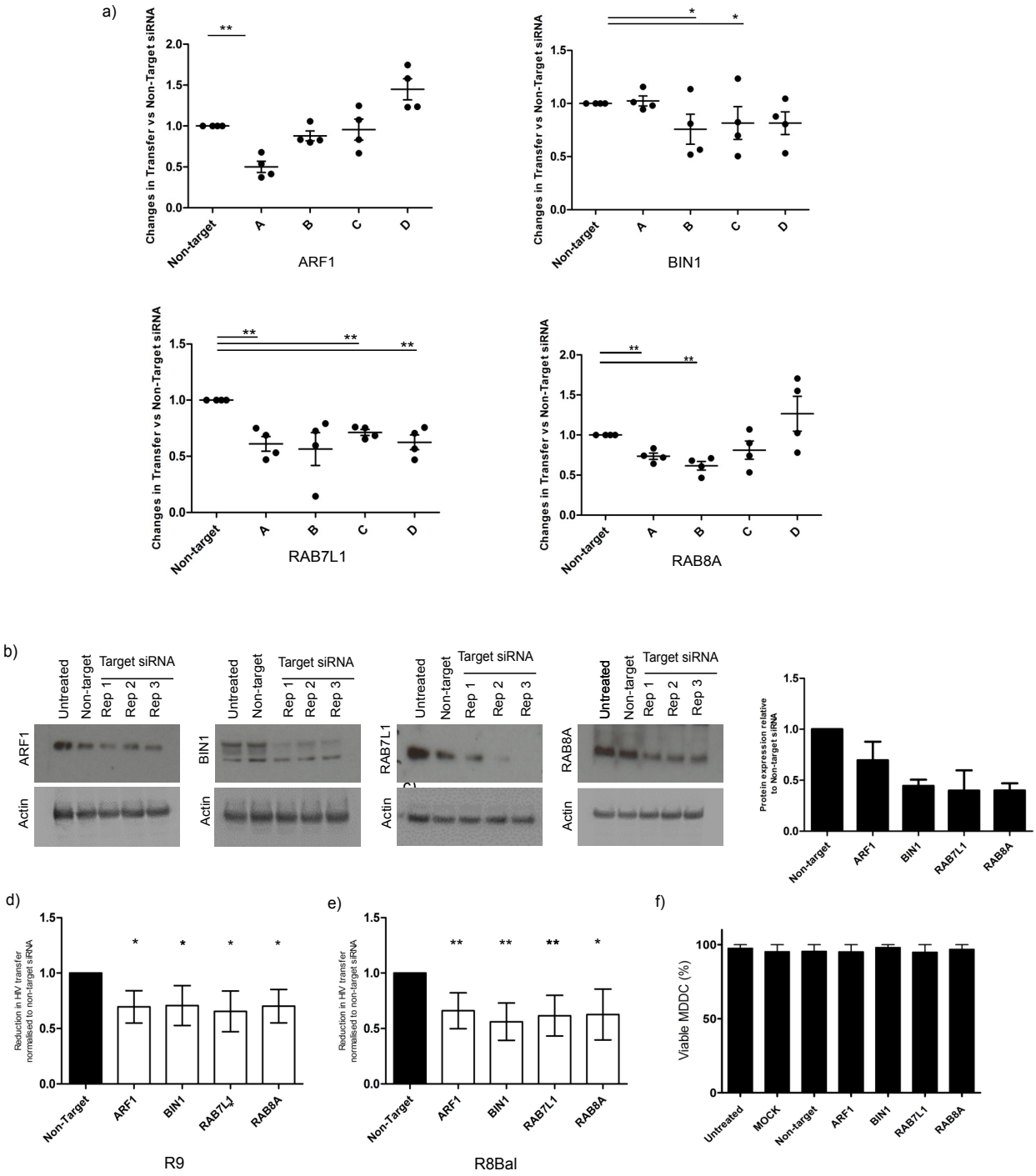

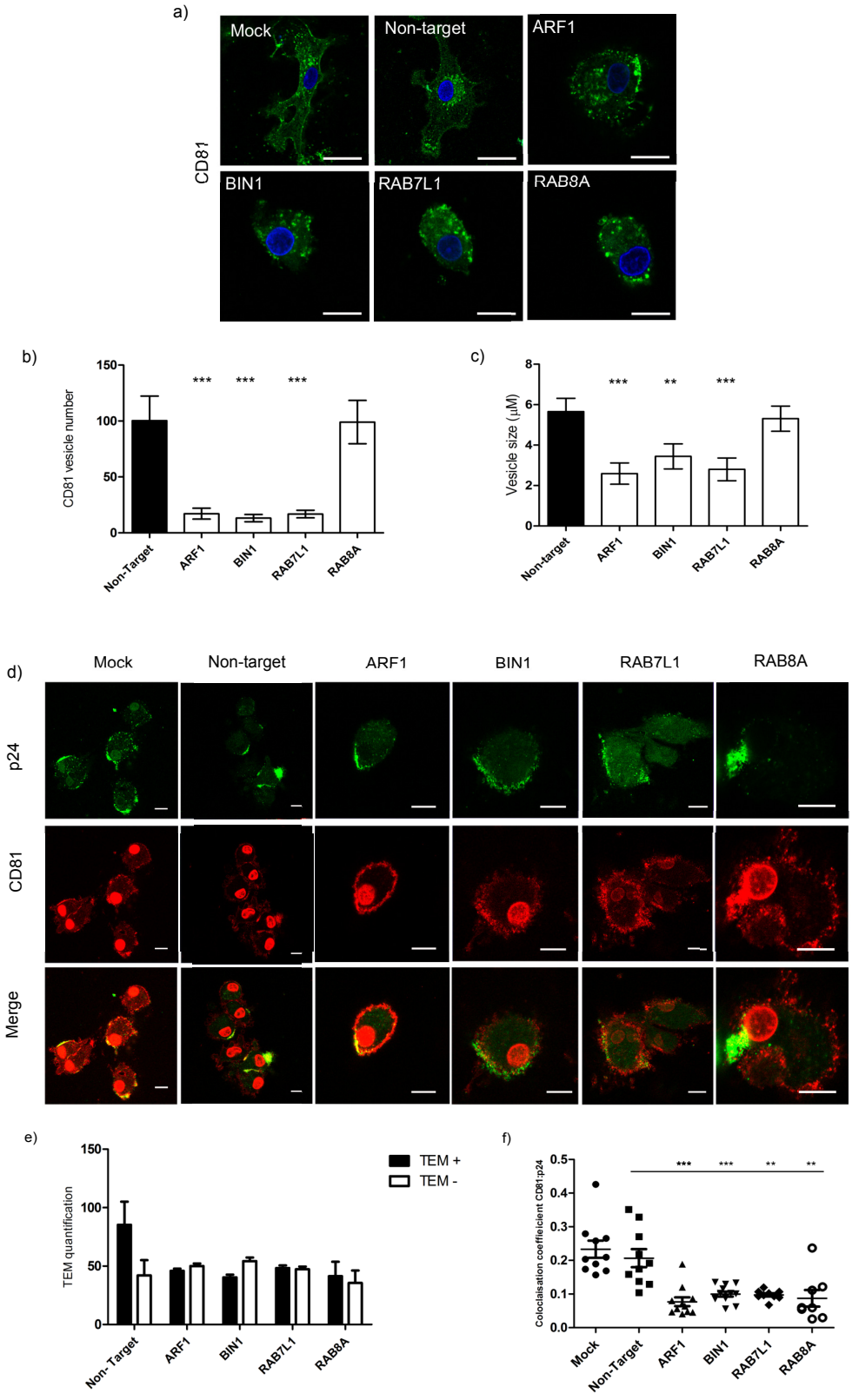

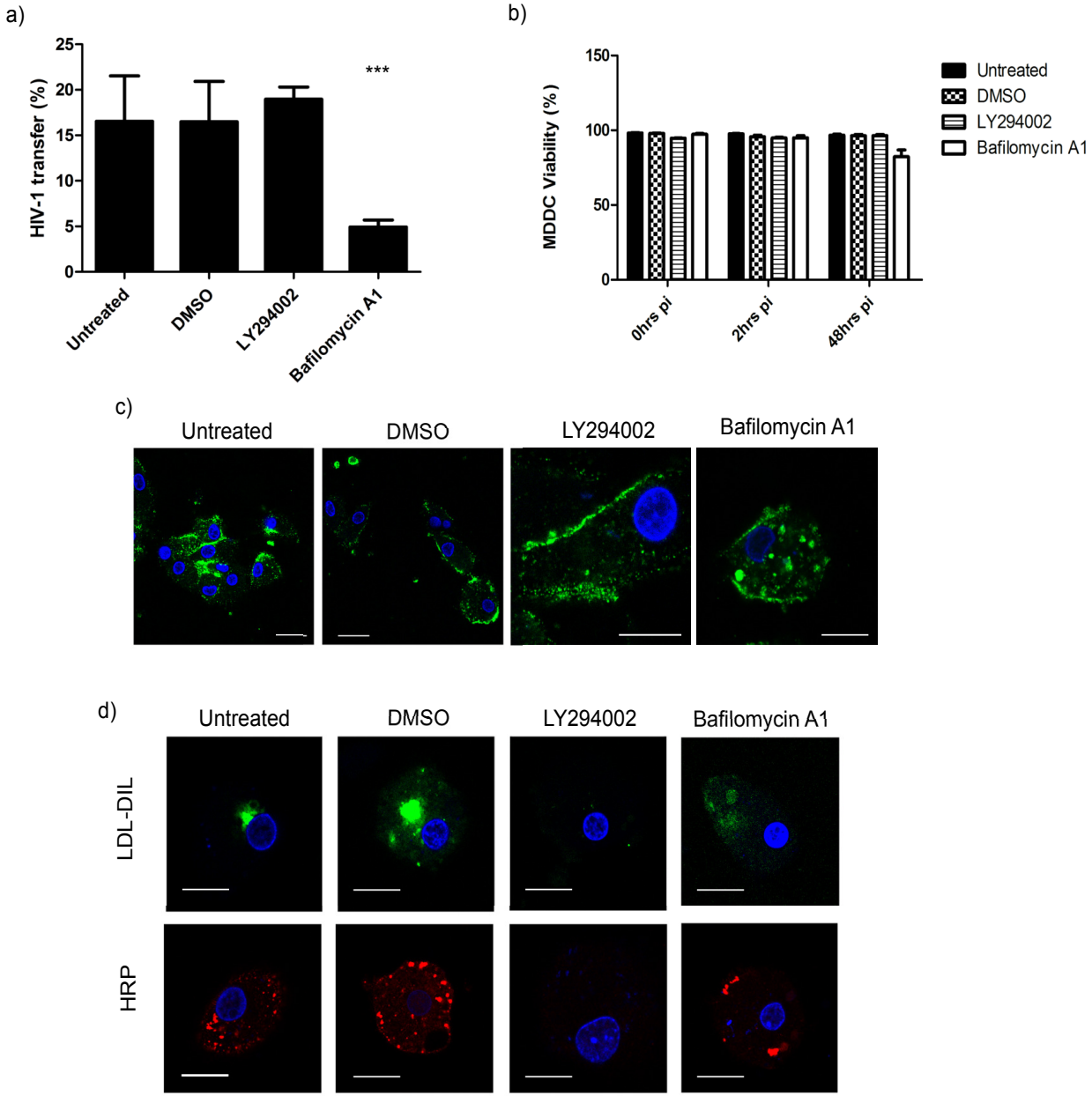

Journal of Virology

JVI

Journal of Virology

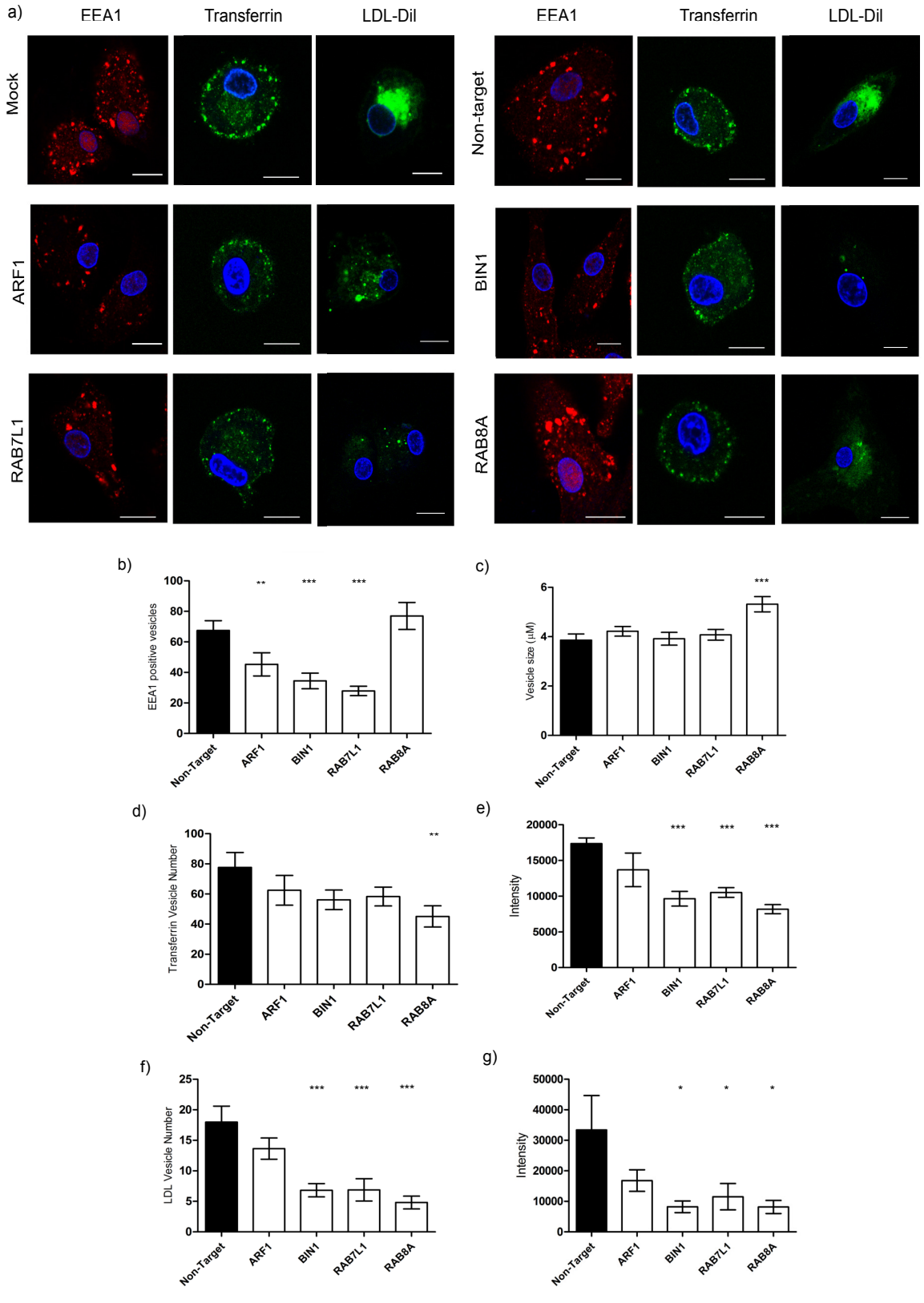

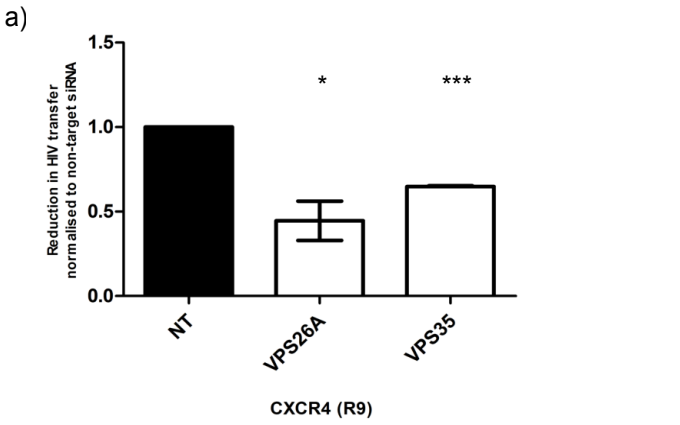

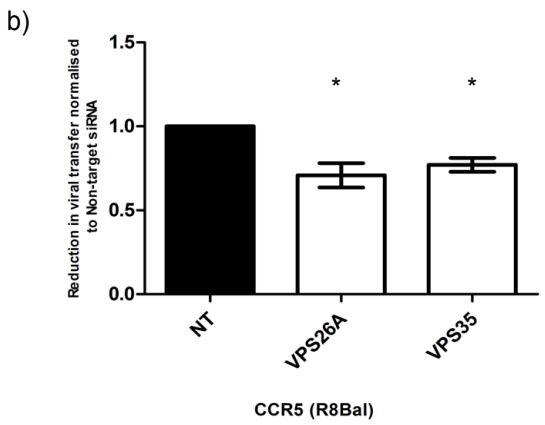

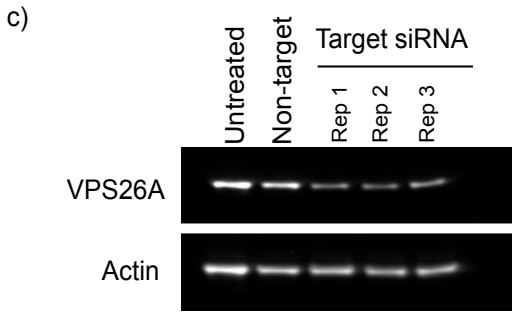

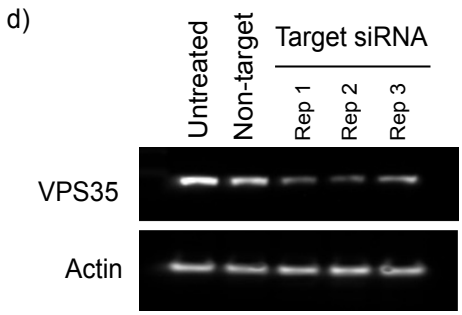

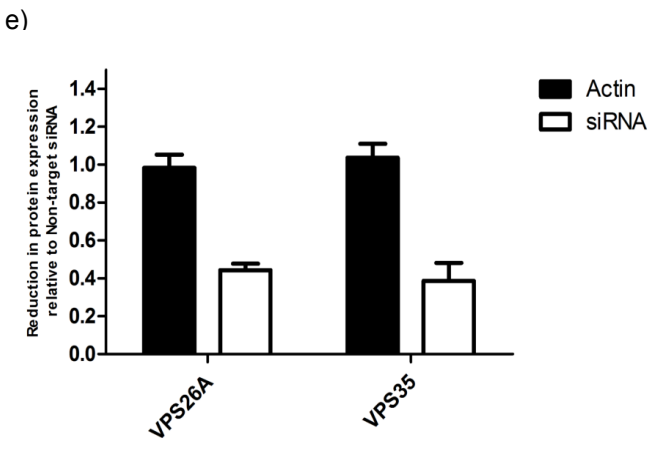

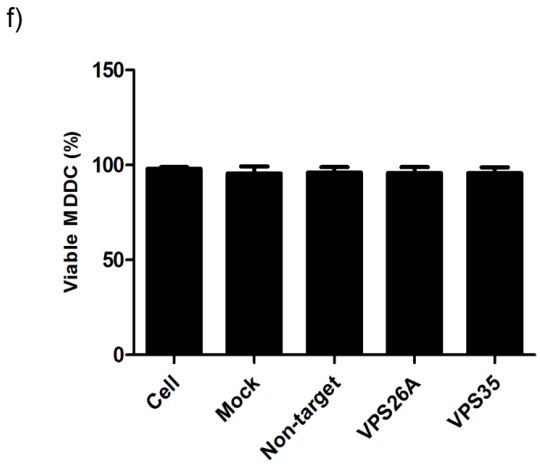

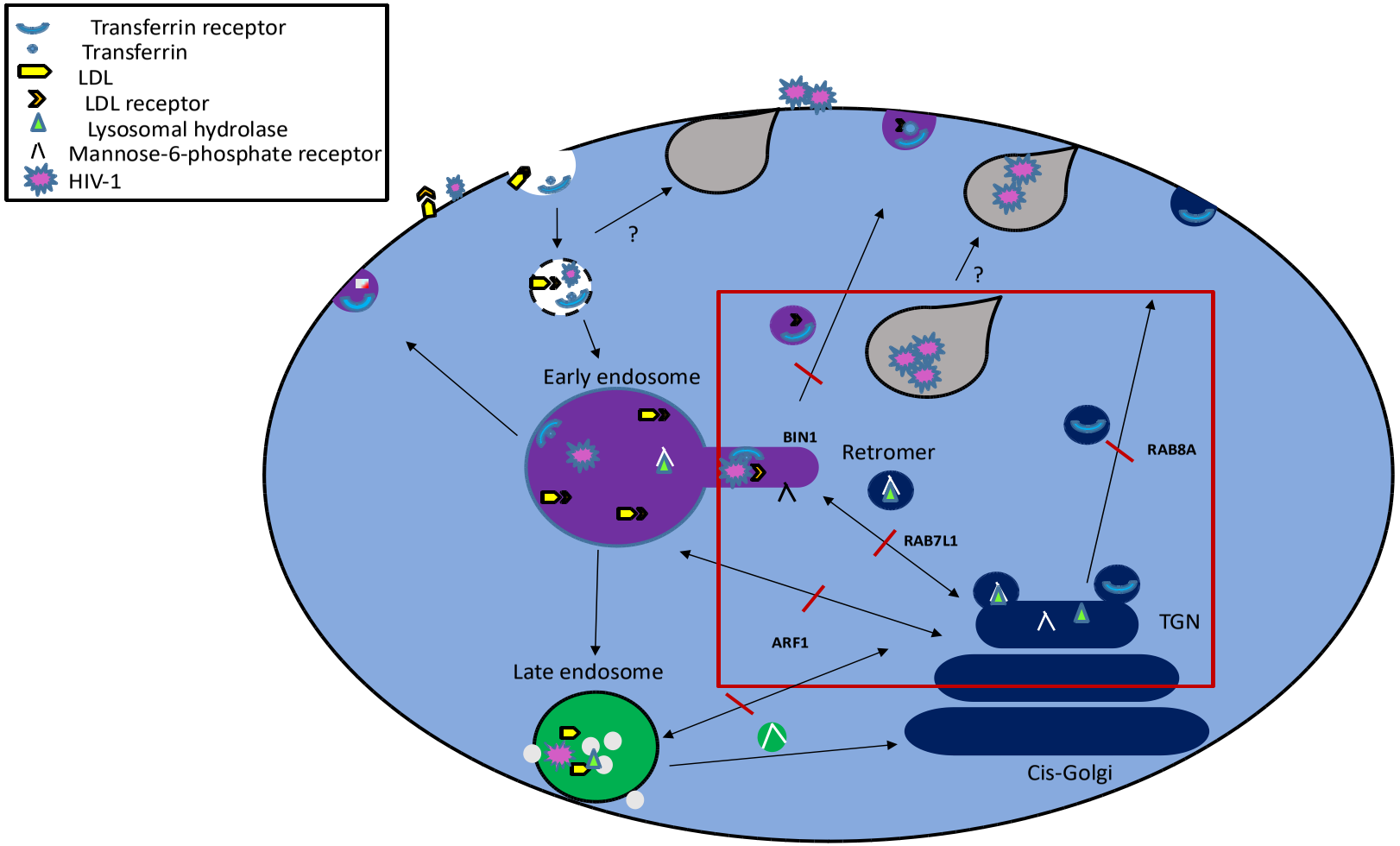

Table 1 Network analysis statistical data

A) Cellular Compartments– Facilitaing Genes			
Nodename	**pvalue**	**qvalue**	**Dataset size**
Cytoplasmic membrane-bound vesicle	1.781257032788977E-5	0.0026505776165784978	7
Cytoplasmic vesicle	2.9736862512104874E-5	0.0022129769452692294	7
Golgi apparatus	7.260275955618954E-5	0.0035995739100488366	7
Clathrin-coated vesicles	1.1280567574068089E-4	0.004193431353399224	4
Trans-Golgi network	1.5015004674908726E-4	0.004464810314555923	4
B) Cellular Compartments– Inhibitory Genes			
Nodename	**pvalue**	**qvalue**	**Dataset size**
Clathrin coat of coated pit	1.98808829214536E-8	2.0278480239444008E-6	4
Clathrin vesicle coat	7.728295638241832E-8	3.9414231596257565E-6	4
Clathrin coat	5.75990999192209E-7	1.9583507854470383E-5	4
Vesicle coat	6.170337924836827E-7	1.5734242778675522E-5	4
Coated pit	1.8932548517714428E-6	3.86216897007019E-5	4
C) Biological Processes – Facilitating Genes			
Nodename	**pvalue**	**qvalue**	**Dataset size**
Vesicle-mediated transport	2.5476631776993885E-7	1.4444208784170076E-4	8
Membrane Orgainisation	7.045745098037326E-5	0.019777204754682143	6
Endocytosis	1.3846610717114176E-4	0.025832390294862395	5
Vesicle Organisation	2.614347913818171E-4	0.03638479278473983	4
Cellular protein localisation	2.906708321191288E-4	0.03242937937435153	6
D) Biological Processes – Inhibitory Genes			
Nodename	**pvalue**	**qvalue**	**Dataset size**
Vesicle-mediated Transport	2.60964598927977E-5	0.011468515190732222	6
Endocytosis	3.158300588098925E-5	0.006955651219872405	5
Receptor-mediated endocytosis	1.0101208431475834E-4	0.0147729914135587	4
Establishment of protein localisation	1.375341659809643E-4	0.015083655172842936	6
Protein localisation	3.4173910866504216E-4	0.02976299308721586	6